JOURNAL OF GEOPHYSICAL RESEARCH, VOL. 115, D00H30, doi:10.1029/2009JD013364, 2010

Click Here for Full Article

Global view of aerosol vertical distributions from CALIPSO lidar measurements and GOCART simulations: Regional and seasonal variations

Hongbin Yu,[1,2,3] Mian Chin,[2] David M. Winker,[4] Ali H. Omar,[4] Zhaoyan Liu,[4,5] Chieko Kittaka,[4,6] and Thomas Diehl[1,2]

Received 9 October 2009; revised 23 February 2010; accepted 26 March 2010; published 24 July 2010.

[1] This study examines seasonal variations of the vertical distribution of aerosols through a statistical analysis of the Cloud-Aerosol Lidar and Infrared Pathfinder Satellite Observations (CALIPSO) lidar observations from June 2006 to November 2007. A data-screening scheme is developed to attain good quality data in cloud-free conditions, and the polarization measurement is used to separate dust from non-dust aerosol. The CALIPSO aerosol observations are compared with aerosol simulations from the Goddard Chemistry Aerosol Radiation Transport (GOCART) model and aerosol optical depth (AOD) measurements from the MODerate resolution Imaging Spectroradiometer (MODIS). The CALIPSO observations of geographical patterns and seasonal variations of AOD are generally consistent with GOCART simulations and MODIS retrievals especially near source regions, while the magnitude of AOD shows large discrepancies in most regions. Both the CALIPSO observation and GOCART model show that the aerosol extinction scale heights in major dust and smoke source regions are generally higher than that in industrial pollution source regions. The CALIPSO aerosol lidar ratio also generally agrees with GOCART model within 30% on regional scales. Major differences between satellite observations and GOCART model are identified, including (1) an underestimate of aerosol extinction by GOCART over the Indian sub-continent, (2) much larger aerosol extinction calculated by GOCART than observed by CALIPSO in dust source regions, (3) much weaker in magnitude and more concentrated aerosol in the lower atmosphere in CALIPSO observation than GOCART model over transported areas in midlatitudes, and (4) consistently lower aerosol scale height by CALIPSO observation than GOCART model. Possible factors contributing to these differences are discussed.

Citation: Yu, H., M. Chin, D. M. Winker, A. H. Omar, Z. Liu, C. Kittaka, and T. Diehl (2010), Global view of aerosol vertical distributions from CALIPSO lidar measurements and GOCART simulations: Regional and seasonal variations, *J. Geophys. Res.*, *115*, D00H30, doi:10.1029/2009JD013364.

1. Introduction

[2] Aerosol can have significant impacts on air quality, weather, and climate. Assessing these impacts requires an adequate, observational characterization of large temporal and spatial variations of aerosol. The emerging capability of satellite remote sensing provides an unprecedented opportunity to advance the understanding of aerosol-air quality-climate linkages. Recent improvements in satellite remote sensing mainly aerosol optical depth (AOD) from passive sensors such as the Moderate resolution Imaging Spectroradiometer (MODIS) [*Remer et al.*, 2005; *Levy et al.*, 2007] and Multiangle Imaging Spectroradiometer (MISR) [*Kahn et al.*, 2005], have resulted in strong observational constraints for the aerosol direct effect on solar radiation at the top-of-atmosphere (TOA) [e.g., *Remer and Kaufman*, 2006; *Yu et al.*, 2004, 2006, 2009]. Satellite AOD data have also been used to enhance the surface air quality monitoring networks for air quality forecast [e.g., *Al-Saadi et al.*, 2005] and to provide observation-based estimates of the long-range transport of aerosol [*Kaufman et al.*, 2005; *Yu et al.*, 2008; *Rudich et al.*, 2008]. However, passive sensors mainly provide total column quantities in cloud-free scenes with little information on the vertical distribution of aerosols except the plume height [*Kahn et al.*, 2007; *Pierangelo et al.*, 2004]. Current assessments of aerosol impacts on climate and air quality remain very uncertain [e.g., *Schulz et al.*, 2006] because the assessments rely largely on model simulations of

[1]Goddard Earth Science and Technology Center, University of Maryland Baltimore County, Baltimore, Maryland, USA.
[2]Laboratory for Atmospheres, NASA Goddard Space Flight Center, Greenbelt, Maryland, USA.
[3]Now at Earth System Science Interdisciplinary Center, University of Maryland, College Park, Maryland, USA.
[4]NASA Langley Research Center, Hampton, Virginia, USA.
[5]National Institute of Aerospace, Hampton, Virginia, USA.
[6]Science System and Applications Inc., Hampton, Virginia, USA.

Copyright 2010 by the American Geophysical Union.
0148-0227/10/2009JD013364

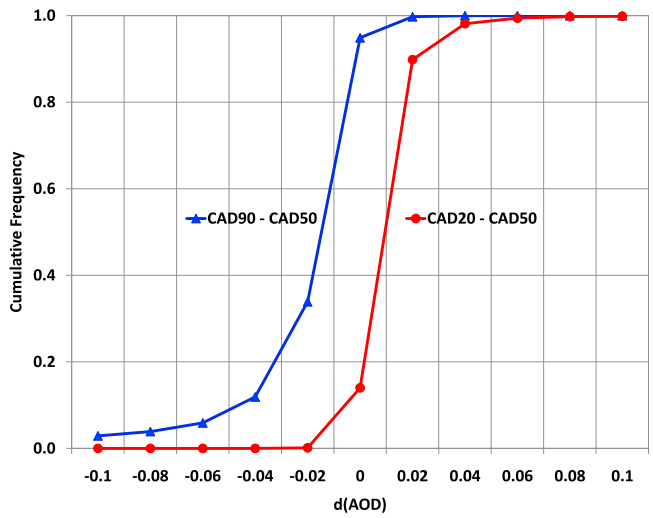

Figure 1. Fractional uncertainty of aerosol optical depth, $\delta\tau/\tau$, resulting from fractional uncertainty of lidar ratio (Fs = δS/S) (following analysis of *Winker et al.* [2009]).

aerosol vertical distributions that differ by up to an order of magnitude among models [*Lohmann et al.*, 2001; *Textor et al.*, 2006].

[3] Because of the recent launch of the Cloud-Aerosol Lidar and Infrared Pathfinder Satellite Observations (CALIPSO), the first-ever, continuous multiyear global aerosol profiling is emerging. This unique capability adds great value to aerosol and cloud research by complementing the increasingly sophisticated passive remote sensing of columnar aerosol (e.g., AOD). It provides an opportunity to assess model simulations of aerosol vertical distributions on global and annual scales. Objectives of this study are to: (1) analyze regional and seasonal variations of vertical distribution of aerosol extinction using CALIPSO lidar observations, and (2) examine differences in aerosol vertical distributions between CALIPSO observations and the Goddard Chemistry Aerosol Radiation Transport (GOCART) model simulations. The real strength in CALIPSO is the high-resolution vertical profile information rather than the AOD, since the latter quantity could be less accurate than that retrieved by passive sensors. Therefore the significant results from this study come from CALIPSO-GOCART comparison of shapes of aerosol extinction profile. Through the statistical analysis of the first observed annual cycle of aerosol vertical distributions on a global scale and comprehensive comparison with the GOCART model, this study complements existing and ongoing validation efforts of CALIPSO measurements [e.g., *Kim et al.*, 2008; *Omar et al.*, 2009] and GOCART simulations of aerosol vertical distributions [*Ginoux et al.*, 2001; *Chin et al.*, 2003] that are usually limited to specific regions and time periods. Different from the first global analysis of the occurring frequency of mineral dust from CALIPSO [*D. Liu et al.*, 2008], this work examines the vertical distributions of aerosol extinction for both dust and non-dust aerosol.

[4] The rest of paper is organized as follows. A brief description of CALIPSO lidar measurements, GOCART simulations, and their major uncertainties is given in section 2. Section 3 describes data screening and sampling techniques, and the broad categorization of dust and non-dust aerosol. In section 4, global patterns and regional variations of aerosol extinction profiles are presented and discussed on a seasonal basis through comparisons of CALIPSO measurements with GOCART simulations and MODIS retrievals of AOD. For conciseness, some items are documented in auxiliary material.[1] Major findings are summarized in Section 5.

2. Brief Descriptions of CALIPSO Lidar Measurements and GOCART Simulations

2.1. CALIPSO Lidar Measurements of Aerosol Vertical Distributions

[5] The CALIPSO mission was launched on April 28, 2006 with an equator-crossing time of about 1:30 P.M. and 1:30 A.M., and a 16-day repeating cycle. The primary instrument onboard the CALIPSO is the Cloud-Aerosol Lidar with Orthogonal Polarization (CALIOP), a two-wavelength, polarization lidar [*Winker et al.*, 2003]. Since June 13, 2006, CALIOP has been collecting almost continuously high-resolution (333 m in the horizontal and 30 m in the vertical in low and middle troposphere) profiles of the attenuated backscatter by aerosols and clouds at visible (532 nm) and near-infrared (1064 nm) wavelengths along with polarized backscatter in the visible channel between 82°N and 82°S [*Winker et al.*, 2007]. Spatial averaging over different scales is usually taken to improve signal-to-noise-ratio (SNR) for reliable aerosol retrieval.

[6] The CALIOP identified features are first classified into aerosol and cloud using a cloud-aerosol discrimination (CAD) algorithm [*Liu et al.*, 2009]. The level of confidence in the aerosol-cloud classification is reflected by a CAD score, which ranges from −100 to 0 for aerosol and +100 to 0 for cloud. A larger absolute value of the CAD score indicates higher confidence of the feature classification. The CALIOP scene classification further associates the aerosol layer with one of six types, namely smoke, polluted continental, polluted dust, dust, clean continental, and clean marine, with respective extinction-to-backscatter ratio or lidar ratio (S) of 70, 70, 65, 40, 35, and 20 sr at 532 nm [*Omar et al.*, 2009]. Details of CALIOP aerosol detection and retrieval algorithms are updated in recent publications [e.g., *Liu et al.*, 2009; *Omar et al.*, 2009; *Young and Vaughan*, 2009; *Winker et al.*, 2009].

[7] Uncertainty associated with the determination of lidar ratio S is one of major factors contributing to the uncertainty of CALIOP aerosol extinction retrieval. The estimated uncertainty [*Winker et al.*, 2009] is shown in Figure 1. Lidar ratio typically varies by about 30% within a given aerosol type. Some types exhibit somewhat more variability and others somewhat less. Misclassification of aerosol type contributes additional uncertainty. At small AOD, the AOD fractional uncertainty can be approximately estimated as the fractional uncertainty of S. However, with an increase of AOD, the fractional uncertainty of AOD is substantially increased. For example, the fractional uncertainty of 30% for S would result in an AOD fractional uncertainty of ~50% for AOD = 0.5 and nearly 100% for AOD = 1. An AOD uncertainty implies an uncertainty in the retrieved profile. For weakly attenuating layers, the shape of the profile is fairly representative,

[1]Auxiliary materials are available in the HTML. doi:10.1029/2009JD013364.

although the magnitude is biased either high or low. For denser layers, retrieval errors tend to accumulate toward the base of the layer, but again the shape of the upper portions of the layer is representative.

[8] Another significant source of uncertainty in the retrieved profile occurs when the base of the aerosol layer is incorrectly identified (most commonly above the true layer base). This happens when the lidar signal is completely attenuated in layers with the optical depth greater than about 3, but can also happen in attenuating aerosol when the detection algorithm incorrectly identifies clear air while still inside the layer. In either case, the AOD is biased low but the error affects only the lower part of the profile.

[9] The CALIOP detection algorithm will miss features with signal below the instrument sensitivity of 2~4 × 10^{-4} $km^{-1}sr^{-1}$ in the troposphere [*Winker et al.*, 2009]. If a lidar ratio of 50 sr is assumed, the minimum detectable extinction coefficient is 1~2 × 10^{-2} km^{-1}. Although the CAD algorithm works well in a majority of cases examined, several specific layer types are prone to misclassification [*Liu et al.*, 2009]. Above or close to source regions, heavy dust or smoke might be misclassified as clouds. Dust transported to the upper troposphere may be misclassified as clouds, which biases the aerosol extinction low. Optically thin clouds in the polar regions may be misclassified as aerosol.

[10] While extensive validation of CALIOP profiles is still going on, several validation efforts have demonstrated that CALIOP has been quite successful in measuring aerosol vertical distributions. Comparisons of simultaneous CALIOP and ground-based lidar over Korea show that the top and base of cloud and aerosol layers are generally in agreement within 0.10 km and the aerosol extinction profiles are generally in agreement within 30% in cloud-free, and nighttime, semi-transparent cirrus cloud conditions [*Kim et al.*, 2008]. Comparisons with the High Spectral Resolution Lidar (HSRL) measurements from two U.S. field campaigns, namely CALIPSO and Twilight Zone (CATZ) and Gulf of Mexico Atmospheric Composition and Climate Study (GoMACCS), show that the CALIOP average extinction biases higher by 0.003 km^{-1} (~20%) and 0.015 km^{-1} (~50%), respectively [*Omar et al.*, 2009].

2.2. GOCART Aerosol Simulations

[11] The GOCART model simulates the major aerosol types, including sulfate, mineral dust, black carbon, organic carbon, and sea salt. The assimilated meteorological fields from Goddard Earth Observing System Data Assimilation System (GEOS DAS) Version 4 are used to drive the GOCART model. The GOCART model has a resolution of 2° latitude by 2.5° longitude in the horizontal and 30 layers in the vertical. Emissions from anthropogenic, biomass burning, biogenic, and volcanic sources and wind-blown dust and sea-salt are included. Other aerosol processes are chemistry, convection, advection, boundary layer mixing, dry and wet deposition, gravitational settling, and hygroscopic growth. Details of GOCART model and evaluation of its results against observations and models are documented in previous publications [e.g., *Chin et al.*, 2000a , 2000b, 2002, 2003, 2004, 2007, 2009; *Ginoux et al.*, 2001, 2004; *Kinne et al.*, 2006; *Textor et al.*, 2006; *Yu et al.*, 2003, 2006, 2009]. Given that the GOCART aerosol vertical distributions have only been evaluated with measurements from lidar [*Ginoux et al.*, 2001] and aircrafts [*Chin et al.*, 2003] over limited regions and seasons, it necessitates a comprehensive evaluation of aerosol extinction profiles using an annual cycle of CALIOP observations in a global scale.

[12] Uncertainties in the GOCART simulations are associated with uncertainties in emissions of individual aerosol types and their precursors, parameterizations of a variety of sub-grid aerosol processes (e.g., wet removal, dry deposition, cloud convection, aqueous-phase oxidation), injection heights of biomass burning smoke and dust, and assumptions on size, absorption, mixture, and humidification of particles. For example, the total dry mass burned from the current biomass burning emission data set is much too low [*Chin et al.*, 2009]. Currently the model assumes that emissions of biomass burning smoke are uniformly distributed in the atmospheric boundary layer (ABL), which may not well represent the reality [*Kahn et al.*, 2008]. In global models, wet removal and convection are parameterized in a simplified way and large diversities among models [*Textor et al.*, 2006] point to major problems in their parameterizations. However, it is extremely difficult to quantify the associated uncertainties. The GOCART aerosol extinction and backscatter are calculated from the Mie theory using prescribed size distributions, refractive indices, and hygroscopic properties of individual aerosol types and assuming external mixing of different types [*Chin et al.*, 2009]. The assumption of spherical particle in the Mie calculation can result in an overestimate of backscatter at 550 nm by a factor of ~2.5 for non-spherical dust [e.g., *Mattis et al.*, 2002; *Liu et al.*, 2002]. In this study, the backscatter from Mie calculations is empirically scaled down by a factor of 2.5.

3. Data Analysis Approaches

3.1. Data Sets and Data Screening

[13] The major data used in this study are CALIOP Level 2 Version 2.01 aerosol layer product from June 13, 2006 to November 30, 2007. The product provides the top and base of aerosol layer, and the layer integrated properties such as extinction AOD, attenuated backscatter (IAB), lidar ratio (S), volume depolarization ratio (VDR), and CAD score, among others.

[14] The analysis focuses on the CALIOP nighttime observations in cloud-free conditions. Because sunlight complicates the aerosol retrieval, the lidar observations at nighttime have higher accuracy than that at daytime. In this study the nominally "cloud-free" profiles are examined, including columns that are completely cloud-free or with the presence of high-level (e.g., cloud base higher than 7 km), optically thin (e.g., cloud optical depth less than 0.1) clouds. The cloud parameters come from the CALIOP 5-km cloud layer product.

[15] Two further data screenings are applied to attain good-quality CALIOP data. One screening is to exclude detected aerosol layers that have low CAD scores. Without specific guideline on setting the CAD score threshold to screen the data, we include the aerosol data with CAD score between −50 and −100 and examine sensitivity of results to the CAD threshold (Figure 2). Setting a more stringent CAD score criteria (e.g., excluding data with the CAD score > −90) reduces the number of sampled cloud-free data profiles and generally the grid and seasonal average AOD. About 60% of

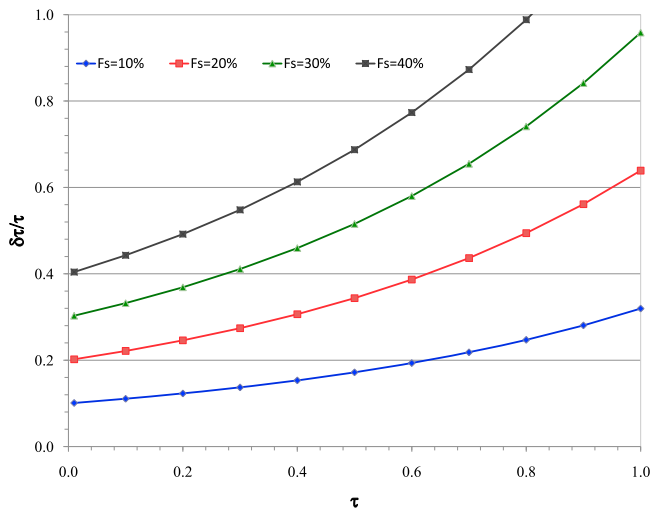

Figure 2. Cumulative frequency of AOD difference [d (AOD)] due to using different thresholds of CAD score to screen the CALIOP data, with blue line representing difference between CAD < −90 and CAD < −50 and red line for difference between CAD < −20 and CAD < −50. The AOD differences are calculated from grid (5° × 4°) and seasonal average CALIOP AOD on a global scale and over the 18-month period from June 2006 to November 2007.

the AOD decrease is within 0.02 and ~80% within 0.04.The AOD decrease of more than 0.1 accounts for only about 3% of the data, which occurs mainly in the "dust belt" extending from the tropical Atlantic northeastward to the northwestern Pacific (roughly from 0° to 50°N and from 50°W to140°E) and in South America and South Africa in biomass burning seasons. Over these regions, the occurrence of dense dust or smoke would yield attenuated backscatter and its color ratio that are more likely to overlap with cloud histograms, resulting in a lower level of confidence of cloud-aerosol discrimination. On the other hand, relaxing the CAD score (e.g., excluding data with the CAD score > −20) increases the number of sampled cloud-free data profiles and generally the grid and seasonal average AOD. 90% of the AOD difference is within 0.02. The choice of CAD score threshold also has small effect on the aerosol scale height (within ± 200 m). Note that CAD > −20 represents some erroneously identified "pseudo-features" that are neither aerosol nor cloud, resulting from the noise of the signal, multiple scattering effects, and overestimate of the attenuation by the overlying layers [*Liu et al.*, 2009].

[16] The other screening is to exclude aerosol layers where the retrieval algorithm has to adjust the initially selected lidar ratio that is based on the type and subtype of the aerosol layer being analyzed. Such adjustment usually occurs for complex features with high AOD that are vertically adjacent to or embedded in other features [*Omar et al.*, 2009]. In such cases, the retrieved AOD and extinction profiles are generally not accurate and the associated uncertainty cannot be reasonably estimated [*Winker et al.*, 2009; *Young and Vaughan*, 2009].

3.2. Separation of Dust and Non-Dust Aerosol

[17] The analysis is performed in the context of aerosol type by taking advantage of the polarization capability of CALIOP. CALIOP allows for the measurements of particulate depolarization ratio (PDR) at 532 nm, a ratio of perpendicular component to parallel component of backscatter by aerosol particles. While non-spherical dust has a typical PDR of 0.1 to 0.4 [*Murayama et al.*, 2001; *Z. Liu et al.*, 2002, 2008; *Mattis et al.*, 2002; *Barnaba and Gobbi*, 2001], spherical particle has a near zero depolarization ratio. Therefore, PDR can be used to effectively distinguish non-spherical aerosol (e.g., dust, volcanic ash) from spherical aerosol (e.g., industrial pollution, biomass burning smoke, and marine aerosol) [*Winker and Osborn*, 1992]. The currently available variable in CALIOP products is the VDR of aerosol layer, which reflects contributions from scattering of both molecules and particulates in a volume to the light polarization. VDR approaches to PDR with high aerosol loading. By following *D. Liu et al.* [2008], we broadly characterize each of CALIOP observed individual aerosol layers as "dust" when VDR is greater than 0.06 or as "non-dust" aerosol otherwise. The individual extinction profiles are aggregated separately into dust and non-dust aerosol to calculate respective regional and seasonal average profiles that are discussed in section 4. In cases where dust mixes with other types of aerosols (e.g., pollution aerosol in India) in the same layer, the simple VDR threshold approach may not work well.

3.3. Comparisons With GOCART and MODIS

[18] The CALIOP data are compared with GOCART simulations of three-dimensional aerosol distributions on global and regional basis. Figure 3 illustrates 12 sections representing distinct aerosol regimes used for the regional analysis. In this study, GOCART results (at 3 h interval) are sampled on the basis of the closest proximity in space and time to the CALIOP cloud free measurements. However, this sampling doesn't guarantee the exact match between GOCART and CALIOP, because of coarse resolutions (2.5° × 2°) of the model and near-zero swath of CALIPSO. We also use MODIS Collection 5 AOD data [*Remer et al.*, 2008; *Levy et al.*, 2007] to evaluate CALIOP and GOCART. To obtain sufficient data coverage, we use a combination of Terra and Aqua MODIS Level 3 daily 1° × 1° data. When both Terra and Aqua aerosol retrievals are available over a grid, an average of them is used. The MODIS data are sampled from a grid encompassing the CALIOP cloud-free observation. Note that while MODIS aerosol measurements are performed during the daytime, CALIOP observations are sampled at night in this study. As CALIOP is the only means that measures nighttime aerosol, it is impossible to assess how the difference in time would complicate the intercomparisons. Here we assume that the difference in time is unlikely to cause significant differences in seasonal average AOD, as suggested by GOCART simulations.

[19] To facilitate the CALIOP-GOCART intercomparison of aerosol extinction (σ) profiles, we define aerosol scale height (H) as an above ground level (AGL) altitude below which 63% of total columnar integration of aerosol extinction (i.e., AOD) is present [*Hayasaka et al.*, 2007], i.e.,

$$\int_0^H \sigma dz = \left(1 - e^{-1}\right) \bullet AOD = 0.63 \bullet AOD \qquad (1)$$

[20] A smaller scale height indicates that aerosol is more concentrated in the lower atmosphere. Although it does not

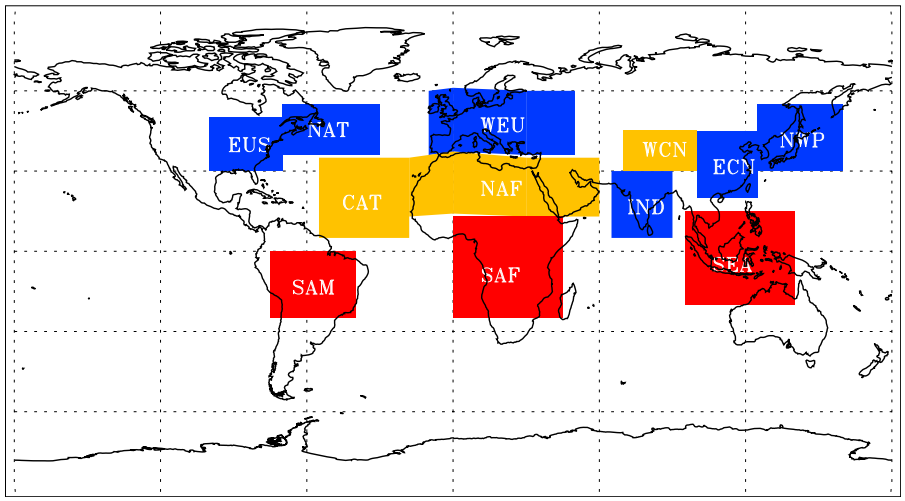

Figure 3. Twelve sections selected for regional analysis in this study, covering source regions of dust (NAF and WCN), biomass burning smoke (SAF, SAM, and SEA), and industrial pollution (EUS, and WEU, ECN, and IND), as well as outflow regions downwind of major dust and industrial pollution sources (CAT, NAT, and NWP). See text for abbreviations.

reflect the detailed layer structures, H in conjunction with AOD provides a useful index for characterizing the aerosol vertical distribution on regional and global scales that involves large volumes of data, in particular for satellite-model and model-model intercomparisons.

4. Results and Discussion

4.1. Global Distributions of AOD and Scale Height

[21] Because of its near-nadir view and the 16-day repeating cycle, a global view of aerosol can only be acquired by averaging the CALIOP cloud-free profiles collected over a period of time (e.g., a month or season) into grid boxes with a horizontal dimension on an order of degrees. In this study we calculate seasonal average cloud-free aerosol extinction and AOD over 5° (longitude) × 4° (latitude) grids with a vertical resolution of 200 m by aggregating CALIOP individual shots of aerosol layers. Figure 4 shows distributions of the number of the nominally cloud-free profiles detected by CALIOP in individual grids. Clean columns where aerosol signal is too weak to be detected by CALIOP are included and the aerosol extinction is set to 0. The detection of cloud-free profile generally occurs more frequently over land than over ocean, consistent with usually higher cloudiness over ocean. The number of the cloud-free profiles is also larger in arid and semi-arid areas than in other areas. Clearly, the number of CALIOP cloud-free aerosol samples is low in such regions as North Pacific, North Atlantic, part of tropical oceans, and Southern Oceans.

[22] Figure 5 shows distributions of cloud-free AOD at 532 nm observed by CALIOP and its comparisons with GOCART simulations and MODIS retrievals at 550 nm for March–April–May (MAM) 2007 and September–October–November (SON) 2007. Similar plots for December–January–February (DJF) 2007 and June–July–August (JJA) 2007 are shown in the auxiliary material. It appears that CALIOP, MODIS, and GOCART give generally consistent spatial patterns of aerosol optical depth and its seasonal variations, with major continental source regions and the trans-Atlantic transport of Saharan dust being readily identified. Several major differences are evident on regional and continental scales. The CALIOP AOD is substantially lower than the GOCART simulation over North Africa and the western China where dust contribution is predominant. Over the Middle East and Indian subcontinent, on the other hand, the CALIOP AOD is higher than the GOCART simulation. Over West Europe, GOCART AOD is higher than CALIOP and MODIS observations. Over major tropical biomass burning regions (e.g., South America, southern Africa, and southeastern Asia in SON and central America in MAM), the CALIOP AOD is higher than the GOCART simulation. One of other most pronounced differences is associated with the intercontinental transport of aerosols. Both MODIS and GOCART show that the trans-Pacific transport of aerosol from East Asia to North America is fairly strong in MAM, with AOD greater than 0.15 over the nearly entire midlatitude North Pacific. However, the CALIOP observations show a much weaker trans-Pacific transport. Similar differences also exist for the trans-mid-Atlantic transport of aerosol from North America to West Europe. On the contrary, the westward transport of aerosol, mainly Saharan dust, by trade winds over tropical Atlantic is stronger and more extended from MODIS and CALIOP observations than the GOCART model. More quantitative comparisons of AOD on regional scales are discussed in the next section in conjunction with comparisons of aerosol extinction profiles.

[23] Global patterns of the scale height for aerosol extinction provide a first order, global view of aerosol vertical distributions. Figure 6 compares global distributions of the seasonal average aerosol scale height derived from CALIOP observations with the GOCART simulations for 2007. Clearly, the GOCART scale heights are consistently higher than the CALIOP observations. The differences are particularly large at the polar regions and northern hemispheric midlatitudes away from the source regions where aerosols are generally transported from outside. The long-range transport of aerosol in these regions is usually associated with midlatitude cyclones that can effectively lift pollution from the atmospheric

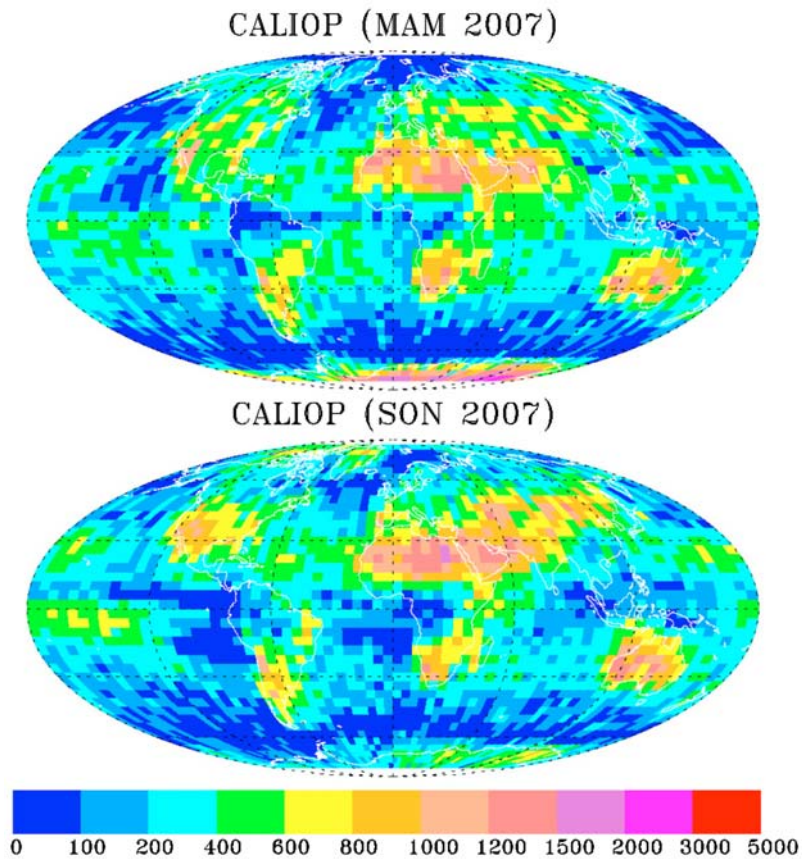

Figure 4. Distributions of the number of nominally cloud-free profiles sensed by CALIOP within each 5° × 4° grid during (top) MAM 2007 and (bottom) SON 2007.

boundary layer (ABL) to the upper troposphere [*Stohl et al.*, 2002]. The much lower CALIOP scale height than the GOCART model in these regions may result from the CALIOP sampling of cloud-free observations that may bias the scale height to low altitudes. CALIOP may miss to detect some optically thin layers in the free atmosphere (FA) because of the detection limit of lidar as discussed in 2.1, resulting in lower scale heights. It is also possible that GOCART model overestimates the vertical transport of aerosols and gives higher scale heights. Nevertheless, both CALIOP observation and GOCART model generally indicate higher scale heights over the dust belt and source regions of biomass burning (e.g., southern Africa and South America) than over industrial pollution source regions and over oceans.

4.2. Regional Profiles of Aerosol Extinction

[24] While aerosol optical depth and scale height provide a useful, first order index of aerosol vertical distribution, detail structures of aerosol extinction cannot be revealed. In the following, we discuss in greater detail the comparisons of seasonal average aerosol extinction and lidar ratio profiles between CALIOP observation and GOCART model over 12 selected regions. Seasonal and regional average lidar ratio S is calculated from individual values of lidar ratio weighted by the aerosol extinction. MODIS AOD is also included in the analysis to evaluate CALIOP retrieval and GOCART model. Although similar plots are made for all regions and seasons, for conciseness we only show plots in 8 representative sections, including eastern U.S. (EUS), eastern China (ECN), Indian subcontinent (IND), North Africa and Arabian peninsula (NAF), central Atlantic (CAT), northwestern Pacific (NWP), southern Africa (SAF) and southeast Asia (SEA) (see Figure 3). Our discussion also focuses on an annual cycle from December 2006 to November 2007. Data from June 2006 to November 2006 are also discussed when significant year-to-year variations are revealed. In the auxiliary material, we document similar plots in 4 other sections and the average AOD and scale height in tables for all sections and seasons.

4.2.1. Source Regions of Industrial Pollution

[25] Major source regions of industrial pollution include the eastern United States (EUS), West Europe (WEU), eastern China (ECN), and Indian subcontinent (IND), of which ECN and IND are also frequently influenced by dust. Figure 7 shows the vertical distributions of seasonal average aerosol extinction and lidar ratio, and comparisons of AOD between CALIOP, GOCART, and MODIS over EUS. z is altitude above ground level (AGL), not mean sea level, throughout the paper. Also shown in Figure 7 are aerosol scale height (H, km) and columnar AOD (τ), with subscript C and G denoting CALIOP and GOCART, respectively. Over eastern U.S., the aerosol extinction from CALIOP and GOCART in the ABL (nominally 0–2 km) agrees in the magnitude, with CALIOP extinction slightly larger than the GOCART counterpart. On the other hand, the CALIOP lidar ratio is generally smaller than GOCART simulations by 10–15 sr (15–20%) in JJA and SON. In the middle to upper part of free atmosphere

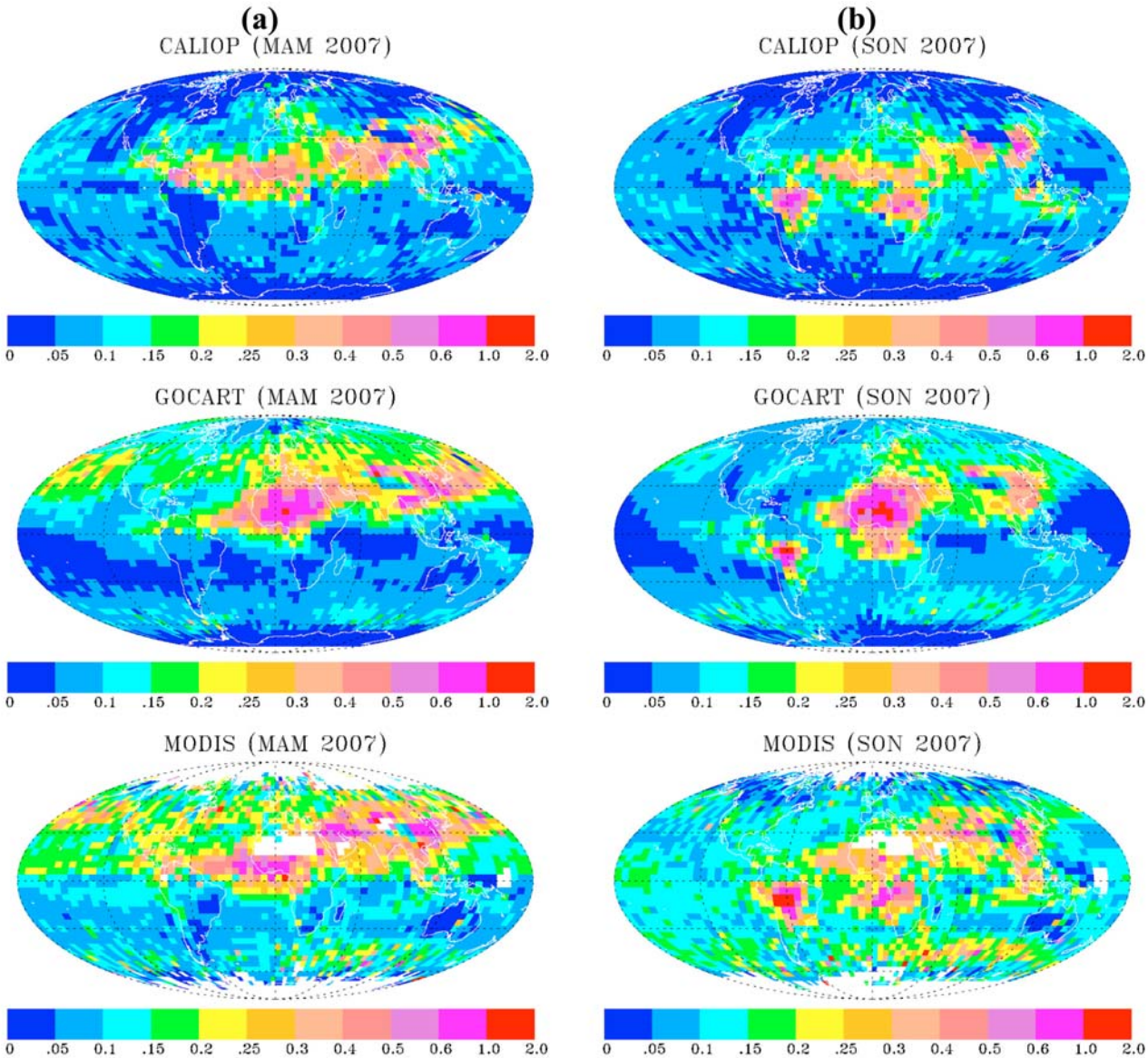

Figure 5. Distributions of seasonal average AOD in cloud-free conditions in (a) MAM 2007 and (b) SON 2007. GOCART simulations and MODIS retrievals are sampled along CALIPSO tracks.

(FA) (generally higher than 4 km), however, the GOCART simulates an aerosol extinction of 0.003 – 0.018 km^{-1}, whereas CALIOP generally doesn't detect aerosol layers presumably because of the detection limit. This gives rise to the much higher scale heights (by 1–2.4 km) from GOCART model than from CALIOP observation, especially in MAM than other seasons. It is also possible that the model overestimates aerosol extinction in the FA. In terms of columnar integration of aerosol extinction or AOD over EUS, CALIOP agrees with GOCART in a range of −45% ~ +20% but is 30–63% consistently smaller than MODIS AOD.

[26] Figure 8 compares CALIOP aerosol extinction profiles with GOCART simulations over eastern China. Except in DJF when CALIOP extinction is slightly higher than GOCART simulation in the ABL, the CALIOP extinction is smaller than the GOCART simulation near the surface and in the FA in other seasons, with the largest difference occurring in MAM and JJA. The aerosol layers (up to 0.04 km^{-1} in MAM) above 4 km as simulated by the GOCART model are not fully observed by CALIOP. As a result, the CALIOP scale height is about 800 m lower than the GOCART model. Again the differences may have resulted from both the possible model overestimate of upward transport and the CALIOP sensitivity limit. Both CALIOP and GOCART suggest that the eastern China (mainly its northern part) is heavily influenced by dust in both seasons, with the dust fraction greater than 0.5 in MAM and DJF and relatively small (0.2~0.35) in JJA and SON. For aerosol lidar ratio, except in DJF when CALIOP agrees with GOCART, CALIOP is smaller than GOCART by 10–20 sr (15–30%) near the surface, with the difference decreasing with increasing altitude. This lidar ratio difference would explain a significant fraction of the AOD difference except in MAM, as can be inferred from Figure 2. In all seasons, the columnar AOD from MODIS is consistently larger than the CALIOP observation and GOCART simulation.

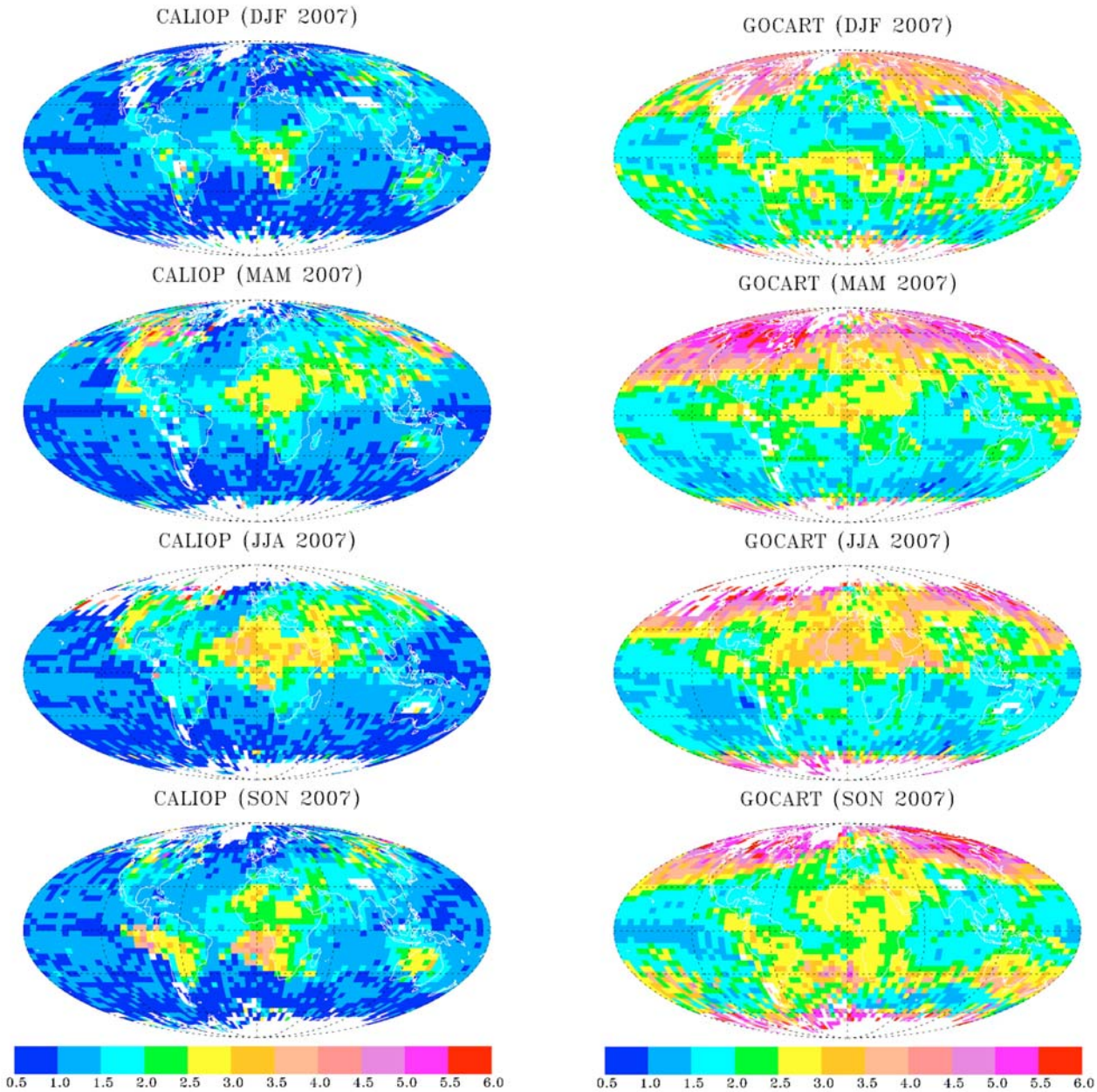

Figure 6. Global patterns of seasonal average scale height (km, above the ground level) of aerosol extinction in cloud-free conditions derived from CALIOP observations and GOCART simulations.

[27] As shown in Figure 9, over the Indian subcontinent (IND) GOCART simulations of total aerosol extinction and AOD are consistently lower than satellite observations. The MODIS AOD can be up to a factor of 2 larger than the GOCART AOD. Except in JJA when CALIOP AOD is smaller than MODIS AOD by a factor of 2, CALIOP and MODIS AODs are generally quite consistent in other seasons. A comparison of GOCART AOD with measurements from Aerosol Robotic Network (AERONET) at Kanpur site in India also shows that the GOCART model underestimates AOD by more than a factor of 2 [*Chin et al.*, 2009]. All these comparisons appear to suggest that the GOCART model tends to underestimate the aerosol optical depth in this region, possibly due to underestimate of emissions. Despite the large CALIOP-GOCART difference in the magnitude of extinction, the general shape of vertical profiles is similar and the scale height of GOCART aerosol extinction is higher than CALIOP observation only by about 340 m on average. Figure 9 also suggests that the CALIOP dust fraction is higher than the GOCART simulation by 0.24 to 0.4. This is qualitatively consistent with the lidar ratio difference between CALIOP and GOCART, with the CALIOP S consistently smaller than the GOCART S by 10–20 sr (15–30%). While the CALIOP observations apparently suggest that the underestimate of GOCART aerosol extinction results mainly from underestimate of dust extinction, comparisons against AERONET observations of spectral dependences of aerosol extinction (Ångström exponent) and single-scattering albedo

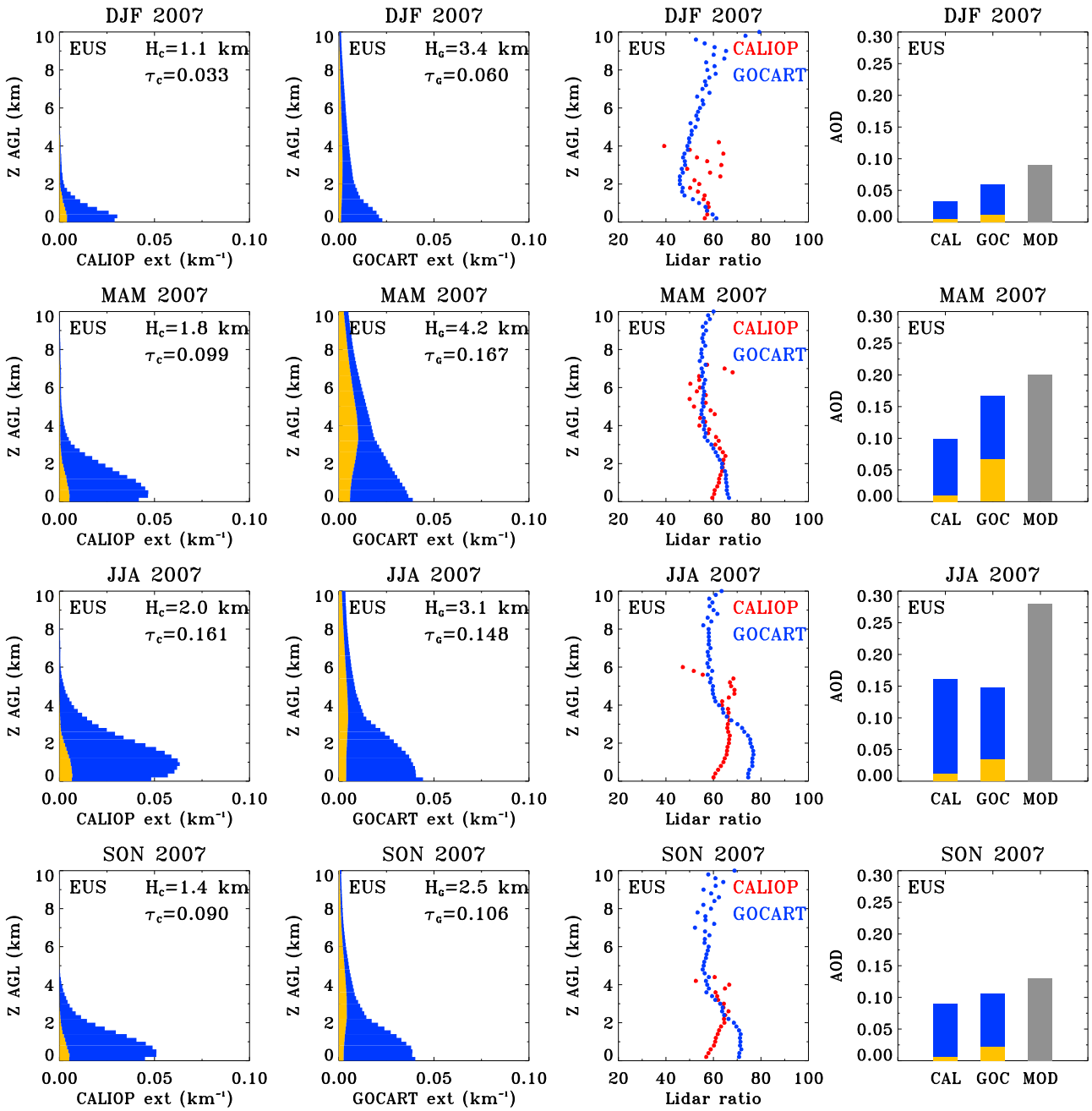

Figure 7. Profiles of seasonal average aerosol extinction coefficient (km^{-1}) and lidar ratio (sr) from CALIOP observation and GOCART model, as well as comparisons of columnar AOD between CALIOP (CAL), GOCART (GOC), and MODIS (MOD) over the eastern U.S. (EUS). Values of aerosol scale height (H) and optical depth (τ) are listed in the extinction profile plots, with subscript C and G representing CALIOP and GOCART respectively. Orange and blue shaded area in extinction profile and AOD plots represents contribution of dust and non-dust aerosol, respectively.

at Kanpur site [*Chin et al.*, 2009] appear to suggest a slight underestimate of dust fraction by GOCART. With in mind that the current VDR threshold approach may not be adequate for an accurate separation of mixed dust and pollution aerosols, a better attribution of the underestimate of extinction to aerosol types requires a more robust separation of dust and non-dust aerosol from satellite measurements. This will provide a better guidance for model improvement.

4.2.2. Source Regions of Mineral Dust

[28] Dust is a predominant component of aerosol over North Africa and Arabian Peninsula (NAF) and the western China (WCN). Figure 10 compares the aerosol extinction profiles from CALIOP and GOCART over NAF. Both CALIOP observation and GOCART model indicate that dust reaches the highest altitude in summer and the lowest altitude in winter, which is consistent with previous studies and is controlled by seasonal variations of turbulent mixing, atmo-

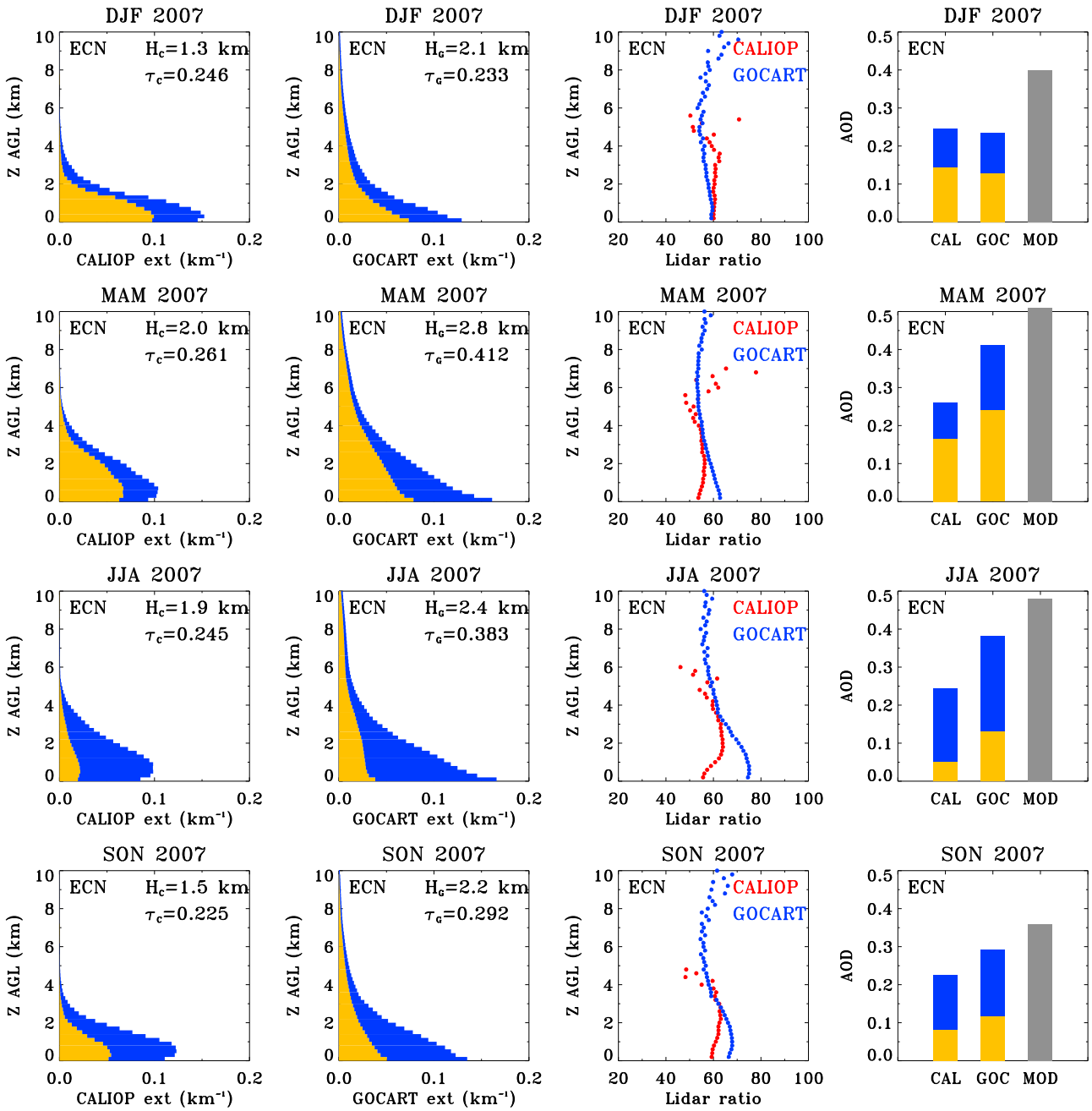

Figure 8. Same as Figure 7 but over the eastern China (ECN).

spheric stability, and circulations [*Kalu*, 1979]. On the other hand, the top of aerosol layer observed by CALIOP is generally 1–2 km lower than the GOCART simulation, due largely to the lidar detection limit. The CALIOP observed aerosol extinction is also much smaller in magnitude with smaller vertical gradient in the lowest 2–3 km layer than the GOCART simulation. Overall the GOCART scale height is 0–0.5 km (0.26 km on average) higher than the CALIOP observation. CALIOP AOD over NAF is smaller than GOCART AOD by about 35% in JJA (both 2006 and 2007) but by more than a factor of 2 in other seasons. Similar CALIOP-GOCART differences exist over WCN (see online auxiliary material).

[29] Several uncertainties or issues associated with both model and satellite can result in the large satellite-model differences in the aerosol extinction. Generally, CALIOP gives the average lidar ratio of 40–45 sr in the region, which is about 5–15 sr (or 10–25%) smaller than GOCART simulated lidar ratio (50–54 sr). It appears that the CALIOP and GOCART dust lidar ratio shown here corresponds respectively to the lower end and higher end of observed dust lidar ratio range of 38–60 [*Tesche et al.*, 2009; *Müller et al.*, 2007; *De Tomasi et al.*, 2003; *Esselborn et al.*, 2009]. As the dust lidar ratio is sensitive to the shape of the non-spherical dust particles, chemical composition, and size distribution [*Barnaba and Gobbi*, 2001; *Liu et al.*, 2002], the observed

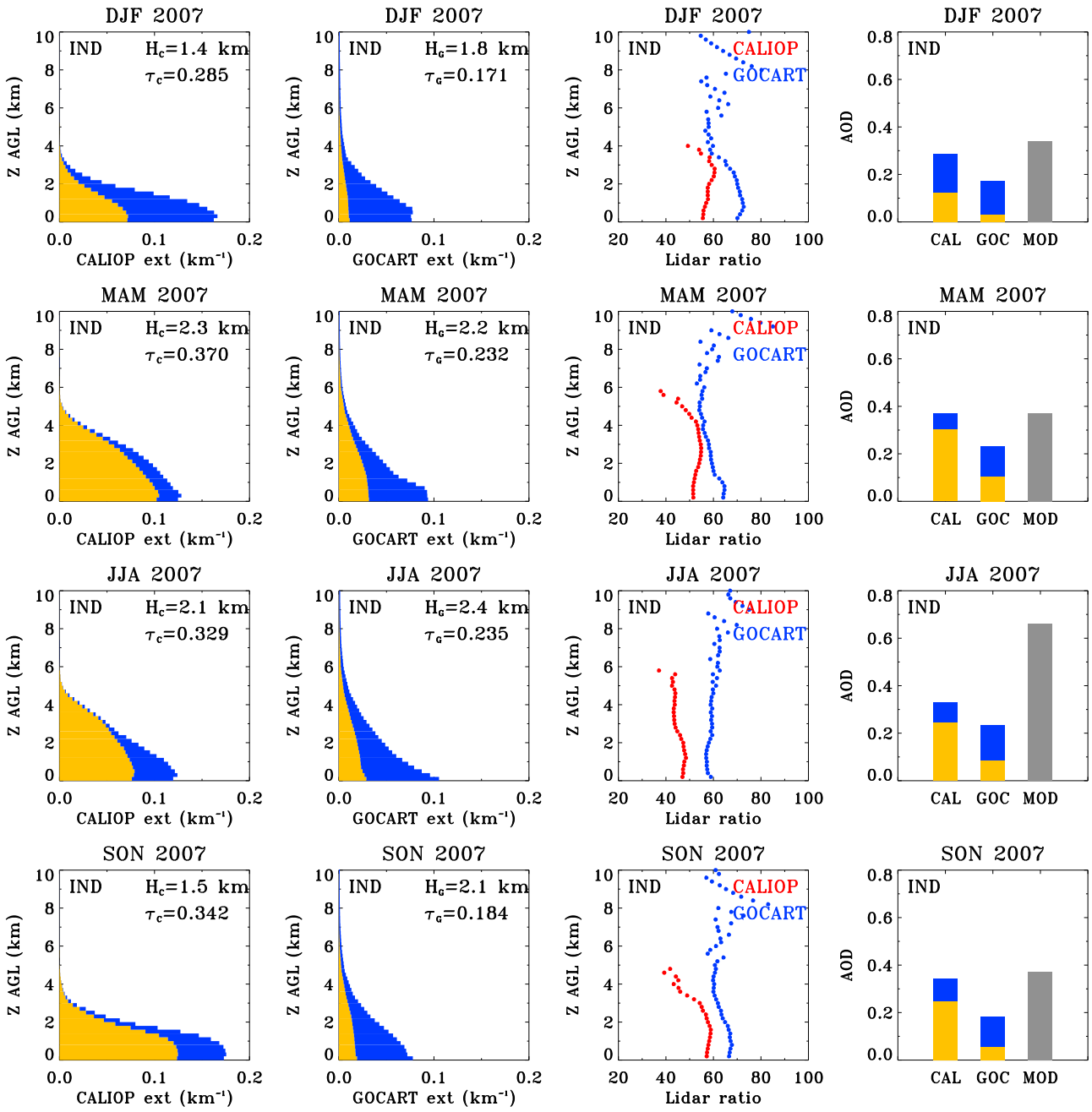

Figure 9. Same as Figure 7 but over the Indian subcontinent (IND).

wide range of lidar ratio may reflect the influence of dust from different source regions [*Esselborn et al.*, 2009].

[30] While the CALIOP-GOCART lidar ratio difference discussed above is consistent with the extinction difference qualitatively, this relatively small difference of lidar ratio is unlikely to fully explain as much as a factor of 2 differences in the extinction. Several other factors would also contribute. For satellite measurements, it remains challenging to distinguish heavy dust loading from clouds, because of the usually large overlap of optical properties between them. As discussed in 2.1, over or close to source regions heavy dust might be misclassified as clouds and also attenuate the light substantially to make the extinction retrieval difficult in lower layers. Both issues bias the aerosol extinction to a lower magnitude and the latter could also shift the height of maximum extinction from near surface to a higher level. From the perspective of model simulations, the GOCART model may have overestimated the source and atmospheric concentration of dust, as suggested by previous model evaluation and intercomparison efforts. The global mean dust emission from GOCART is at the high end among 16 models that participated in the Aerosol Comparisons between Observations and Models (AeroCom) [*Textor et al.*, 2006]. Although comparisons of GOCART AOD with AERONET measurements show small positive bias (14%) of GOCART averaged over the NAF region [*Chin et al.*, 2009], the AERONET sites are mostly concentrated in the southern part of NAF region or at the coastal line in the northern NAF. So it is not clear how

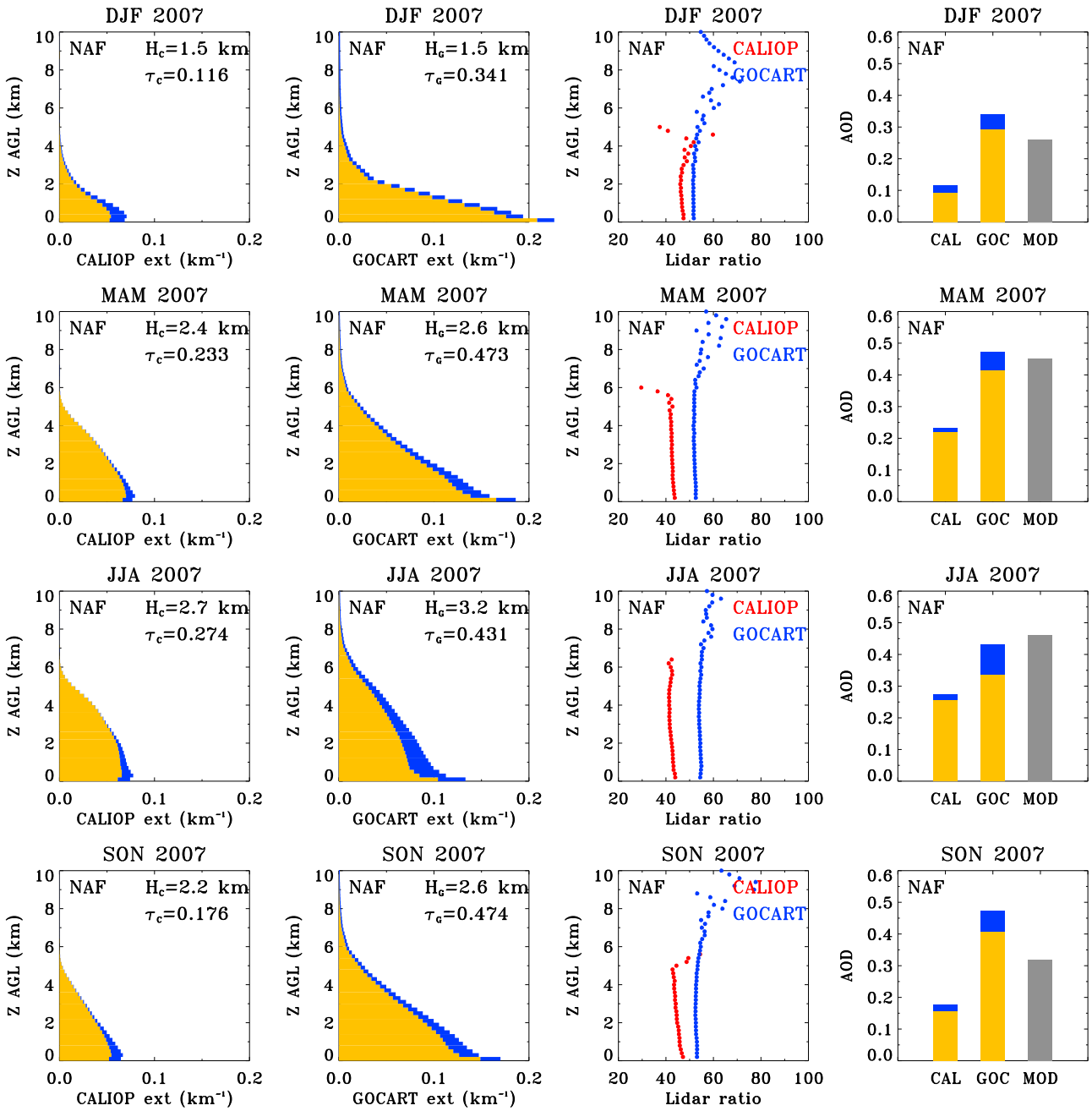

Figure 10. Same as Figure 7 but over North Africa and Arabian Peninsula (NAF). Note that because of missing MODIS retrievals over deserts, MODIS AOD is not directly comparable to CALIOP and GOCART averages.

the GOCART model performs in the inland of the northern NAF because of lack of AERONET observations. As clearly shown in Figure 5, differences between the CALIOP observation and GOCART model are larger in northern NAF than in southern NAF.

4.2.3. Outflows Downwind of Major Dust and Industrial Pollution Source Regions

[31] The central Atlantic Ocean (CAT) is substantially influenced by dust from North Africa around a year and to some extent by biomass burning smoke from the tropical Africa in northern hemispheric winter. As shown in Figure 11, both CALIOP and GOCART consistently indicate that dust is transported in both the ABL and free atmosphere, although the fraction of dust in the marine ABL is lower because of the existence of marine aerosol. Both the observation and model also show that dust layer is transported at higher altitudes in summer than in winter. This is consistent with previous observations [*Kalu*, 1979; *Chiapello et al.*, 1997]. Unlike the large differences over the upwind source region (NAF) as discussed earlier, CALIOP and GOCART extinction profiles and AOD show much better agreement in this dust outflow region. Both CALIOP and GOCART AODs are generally smaller than MODIS AOD. Differences in lidar ratio are also

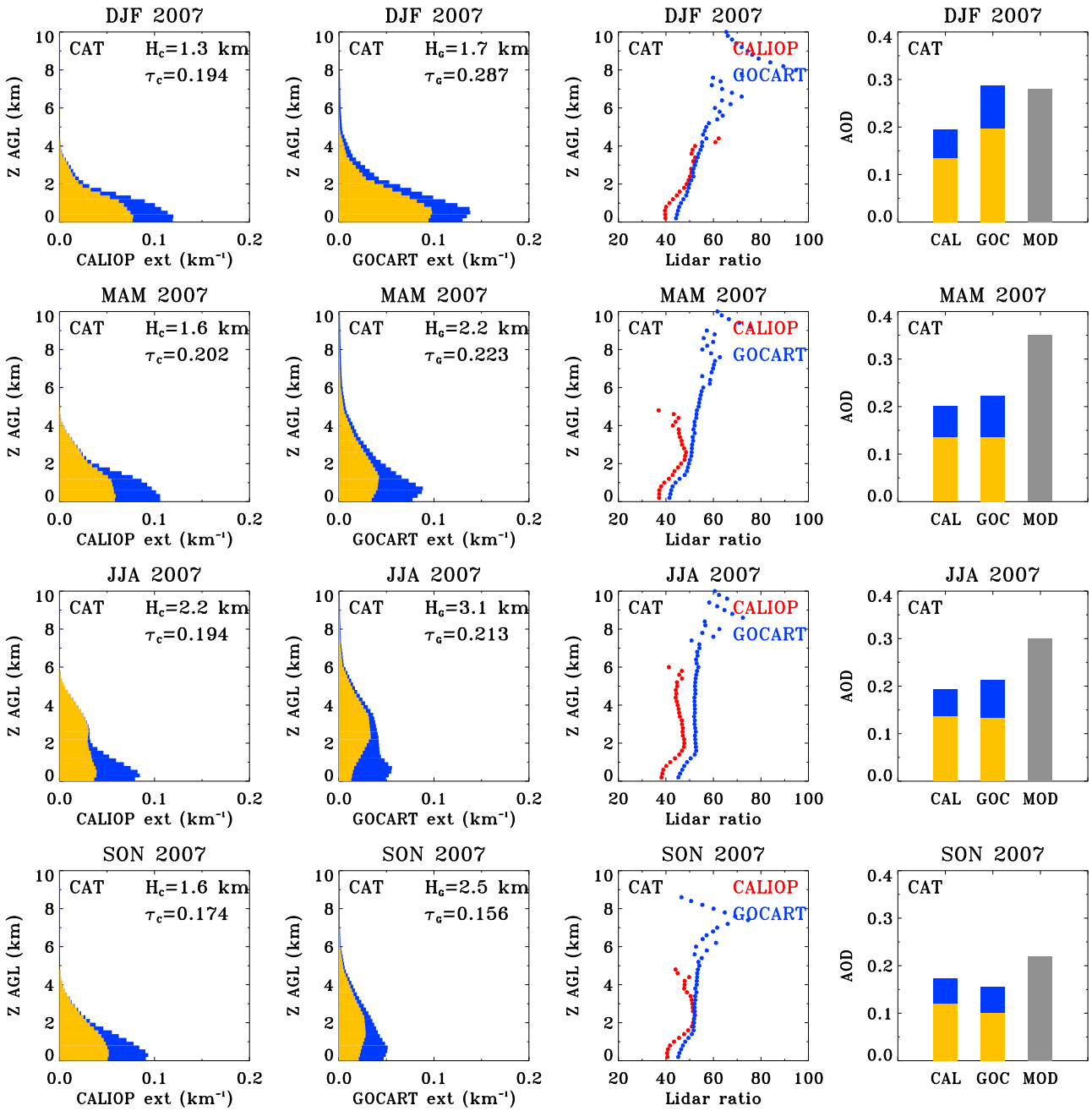

Figure 11. Same as Figure 7 but over the central Atlantic (CAT).

small with the CALIOP values being < 10 sr (or 10–20%) lower than the GOCART simulations.

[32] On the contrary, substantial differences exist between CALIOP observations and GOCART simulations for both the East Asia outflows over the northwestern Pacific (NWP, Figure 12) and North America outflows over the midlatitude North Atlantic (see online auxiliary material). CALIOP AOD is lower than GOCART (and also MODIS) AOD by more than a factor of 2, except in DJF (December–January–February) when the difference is much smaller. The large AOD differences result mainly from differences of aerosol extinction above the ABL. CALIOP rarely detects aerosol layers above 4 km, whereas GOCART simulations show consistent and considerable outflow of dust and non-dust aerosols throughout the FA. Although CALIOP did detect some aerosol layers between 4 and 6 km in MAM 2007, the observed magnitude of aerosol extinction was substantially smaller than the GOCART model. Seasonal average scale heights from the GOCART model range from 3.2 to 4.3 km, which is 1.2–2.3 km higher than CALIOP observations. Aerosol scale heights as inferred from several ground-based lidar observations under cloud-free conditions in the region appear to agree better with CALIOP observations than with GOCART simulations. For example, *Hayasaka et al.* [2007] reported a wide range of scale height from 0.5 to 6 km over three Japanese sites in MAM 2005, of which about 80% are between 1.0 and 4.0 km and a smaller scale height generally corresponds to a larger AOD. *Nakajima et al.* [2007] reported

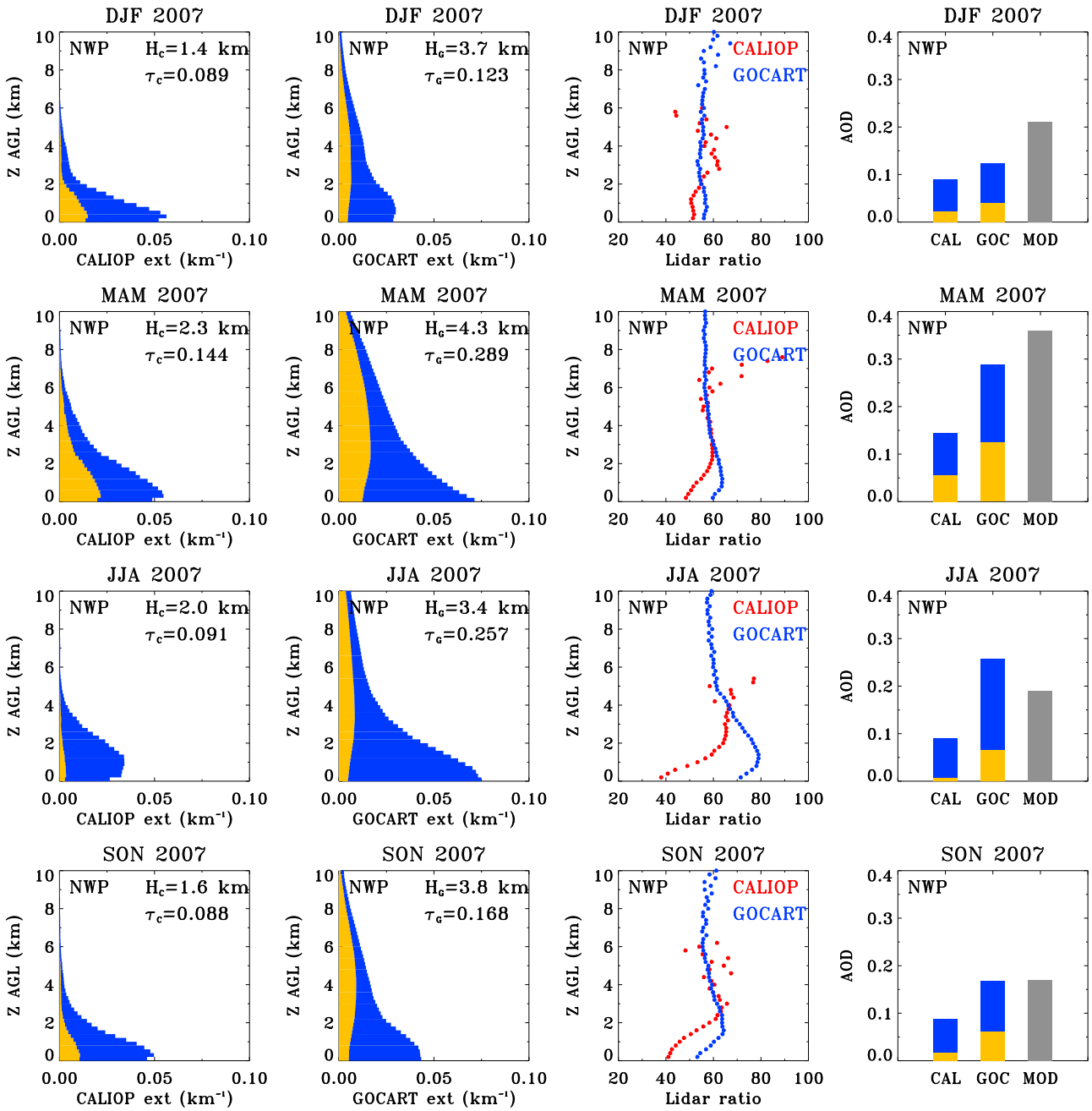

Figure 12. Same as Figure 7 but over the northwestern Pacific (NWP).

the smaller scale height of 1–1.5 km during the same period. Observations over two Japanese sites in spring 2001 suggest that the scale height is 2–3 km for dust and 1–2 km for non-dust aerosol [*Shimizu et al.*, 2004]. Multiyear lidar observations over the Korean peninsula suggest that the scale height is about 2 km in spring, somewhat higher in summer and lower in winter and autumn [*Kim et al.*, 2007]. On the other hand, the aircraft measurements of dust during the Aerosol Characterization Experiment (ACE)–Asia field experiment in spring 2001 shows a persistent feature of dust peaks at 4–5 km over the Yellow Sea and the Sea of Japan, which is well reproduced by GOCART model [*Chin et al.*, 2003].

[33] The large differences between observations and model could result from several factors associated with both satellite and model. MODIS observation in this region is prone to cloud contamination and can be complicated by the presence of non-spherical dust in the region [*Remer et al.*, 2005]. GOCART model may have overestimated dust emissions and the aerosol transport to FA, as discussed earlier. From the perspective of CALIOP observations, the lidar detection limit may have biased both the extinction and scale height lower. There may be possible misclassifications in CALIOP aerosol sub-typing and aerosol-cloud discrimination. As discussed in 2.1, dust aerosol transported to the upper troposphere tends to be misclassified as thin cirrus clouds, resulting in somewhat underestimate of the aerosol extinction. As shown in Figure 12, the CALIOP lidar ratio in the marine ABL is generally much smaller than the GOCART simulation (in

particular in summer). As described by *Omar et al.* [2009], a feature is classified as polluted continental aerosol only when IAB is less than 0.01 and the depolarization is between 0.05 and 0.075. When depolarization ratio < 0.05 or IAB > 0.01, the feature is classified as marine aerosol. As marine aerosol and polluted continental aerosol have similar depolarization ratios, this simple threshold approach may not work well. For high aerosol loading with IAB > 0.01 the feature is exclusively classified as marine aerosol, while the layer is more likely to be polluted continental aerosol. A statistical analysis shows that in the lowest 1km layer over the ocean, CALIOP characterizes aerosol features as marine aerosol at a respective frequency of 27% (DJF), 39% (MAM), 63% (JJA), and 55% (SON). The seasonality of marine aerosol detection frequency is consistent with that of lidar ratio discrepancy as shown in Figure 12. Given that marine aerosol has a lidar ratio of 20 sr that is smaller than that for continental pollution by a factor of ~3, a substantial underestimate of aerosol extinction can be resulted from a misclassification of polluted continental aerosol as marine aerosol in coastal areas where ABL pollution outflow occurs frequently.

[34] The other probable factor is that CALIOP cloud-free observations discussed above may not be representative of GOCART simulations and MODIS observations. The outflows of pollution or pollution/dust mixture in northwestern Pacific Ocean (NWP) and northern Atlantic Ocean (NAT) are usually associated with midlatitude cyclones [*Stohl et al.*, 2002]. GOCART simulations represent averages over 2.5° × 2° grids, including both clear and cloudy conditions. MODIS with a resolution of 500 m and nearly daily global coverage can sample areas close to cloud systems quite frequently. While CALIOP can sample in the vicinity of clouds because of its high spatial resolution, its single-nadir view and 16-day repeating cycle makes such sampling much less frequently. It is possible that the analysis of CALIOP cloud-free measurements as in this study (and ground-based lidar measurements too) may have missed some intense transport events associated with cloudy conditions. CALIOP does have a capability of detecting aerosols above the low-level clouds if high-level clouds are optically thin. Over NWP, CALIOP detected AOD above low-level clouds (with an average cloud top of about 1.5 km above the surface) is 0.07 for MAM, 0.046 for JJA, and 0.033 for DJF and SON. These above-cloud AODs differ from the cloud-free above −1.5 km AODs by less than 25% and are about 37–50% of cloud-free total columnar AOD. While these above-cloud AODs are significant in magnitude in comparison with the cloud-free values, it remains difficult to assess to what extent the exclusion of CALIOP observations in cloudy conditions contributes to the large differences between CALIOP and GOCART or MODIS because of lack of observations of aerosols below optically thick clouds.

4.2.4. Source Regions of Biomass Burning Smoke

[35] The southern Africa (SAF) region defined in Figure 3 encompasses biomass burning sub-regions shifting with season: the Sahel region adjacent to the Sahara deserts with peak burning in DJF and the southern Africa with peak burning in JJA and SON. The region is also influenced by dust to some degree, because the predominant northerly to northeasterly flow over the Sahara deserts in the northern hemispheric winter can transport Saharan dust to the Sahel and the gulf of Guinea [*Kalu,* 1979]. As shown in Figure 13, the lowest aerosol extinction occurs consistently in MAM from both CALIOP observation and GOCART model. GOCART simulates the highest extinction in DJF, which is about a factor of 2 larger than that in JJA and SON. On the other hand, CALIOP observations show no discernable difference between DJF, JJA and SON. As such the most pronounced CALIOP-GOCART differences occur in DJF. The GOCART AOD in DJF is about 60% higher than measurements from both CALIOP and MODIS. The smoke layers between 4 and 6 km as calculated by the GOCART model are not observed by CALIOP. In other seasons, the model simulations of extinction and AOD agree with the satellite measurements within 10–30%. Another notable, consistent feature in Figure 13 is a considerably large fraction of dust extinction in DJF and MAM, and a minimum dust fraction of less than 10% in JJA. The CALIOP observations suggest that the southward transport of Saharan dust imports AOD of 0.144 and 0.072 into the SAF region in DJF and MAM, respectively, which is more or less equivalent to the non-dust AOD in the region. For comparisons, GOCART yields nearly the same dust AOD (i.e., 0.146 and 0.077 for DJF and MAM, respectively) and comparable percentile contribution of dust AOD (37% and 55%, respectively). The lower dust fraction (37%) of GOCART AOD in DJF results from much higher non-dust AOD calculated by the model than observed by CALIOP. For lidar ratio, CALIOP generally agrees with the model to within ± 10 sr.

[36] Figure 14 shows comparisons of aerosol extinction between CALIOP observation and GOCART model over South America (SAM) during peak biomass burning season (SON). As clearly shown in Figure 14, a significant amount of smoke aerosol is pumped above the ABL (over Amazon basin during the dry season, the convective ABL in the afternoon reaches ~1 km over forest and ~1.6 km over pasture, *Fisch et al.*, 2004). The analysis is consistent with other measurements [*Andreae et al.*, 2004; *Yu et al.*, 2007]. For 2006, the GOCART AOD of 0.12 is about 50% smaller than the CALIOP and MODIS observations (AOD = 0.21 and 0.24, respectively). This may suggest possible underestimate of biomass burning emissions by GOCART model. On the other hand for 2007, the agreement between CALIOP and GOCART are reasonably good, except for the altitude of the largest aerosol extinction. While the CALIOP observation shows the largest extinction at 2 km, the GOCART model gives the largest extinction near the surface. One probable reason for this difference is that the attenuation of CALIOP signal would miss the detection of smoke near the surface, as discussed in section 2.1. For columnar AOD, both CALIOP and GOCART are nearly 50% smaller than the MODIS AOD of 0.46.

[37] Figure 14 also shows significant interannual variability of biomass burning aerosol in the region. The biomass burning emissions of carbonaceous aerosol used in GOCART is about a factor of 3 higher in 2007 than 2006. For both GOCART and MODIS, AOD in 2006 is about half of that in 2007. Previous study also shows that MODIS AOD in 2006 is about a half of that in 2005 [*Koren et al.*, 2007]. The sharp decrease of biomass burning emission in 2006 is linked to the implementation of a tri-national policy on burning control in the region [*Koren et al.*, 2007]. However, CALIOP reveals a much smaller interannual variability, with AOD being 33% lower in 2006 than 2007, which would at least be linked partly

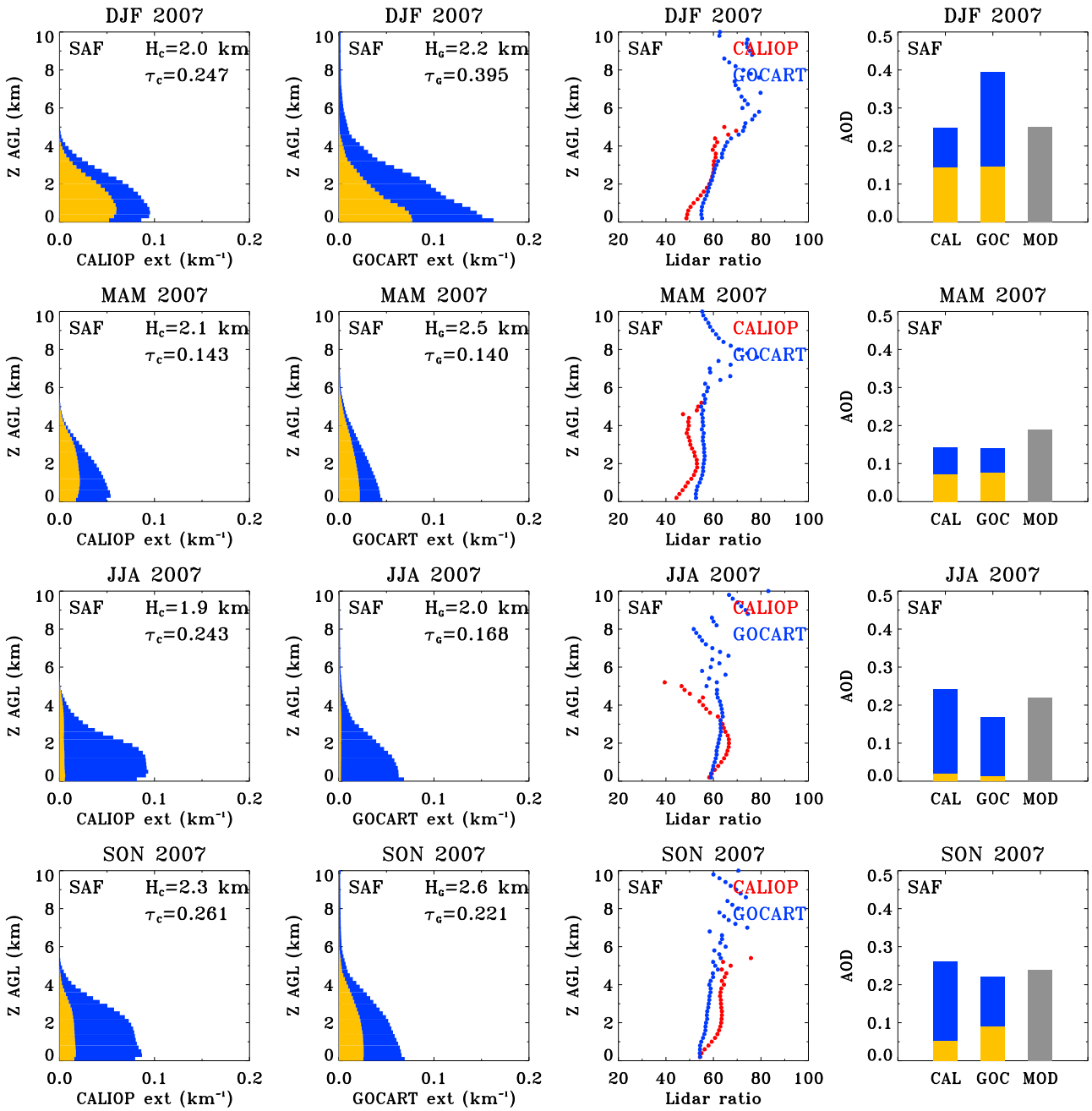

Figure 13. Same as Figure 7 but over the southern Africa (SAF).

to the uncertainty associated with laser attenuation by heavy smoke. The stronger attenuation of laser makes the smoke in the ABL less detectable by lidar in 2007, as corroborated by the elevation of height of maximum extinction from about 0.5 km in 2006 to 2 km in 2007.

5. Summary and Conclusions

[38] We have performed an analysis of three-dimensional distributions of seasonal average aerosol extinction at 532 nm by using CALIPSO lidar measurements in cloud-free night-time conditions from June 2006 to November 2007. CALIOP measurements of aerosol extinction are compared with GOCART model simulations and MODIS AOD observations. Our analysis shows reasonably good agreements between satellite observations and model simulations, including:

[39] 1. In general, CALIOP observations of geographical patterns and seasonal variations of aerosol optical depth are consistent with GOCART simulations and MODIS retrievals, in particularly in source regions.

[40] 2. Both CALIOP observation and GOCART model show that the aerosol scale heights in dust and smoke source regions are higher than that in industrial pollution source regions, though the scale height calculated by GOCART model is consistently higher than CALIOP observation.

[41] 3. Satellite observations and model simulations give a generally consistent characterization of both magnitude and altitude of trans-Atlantic transport of Saharan dust.

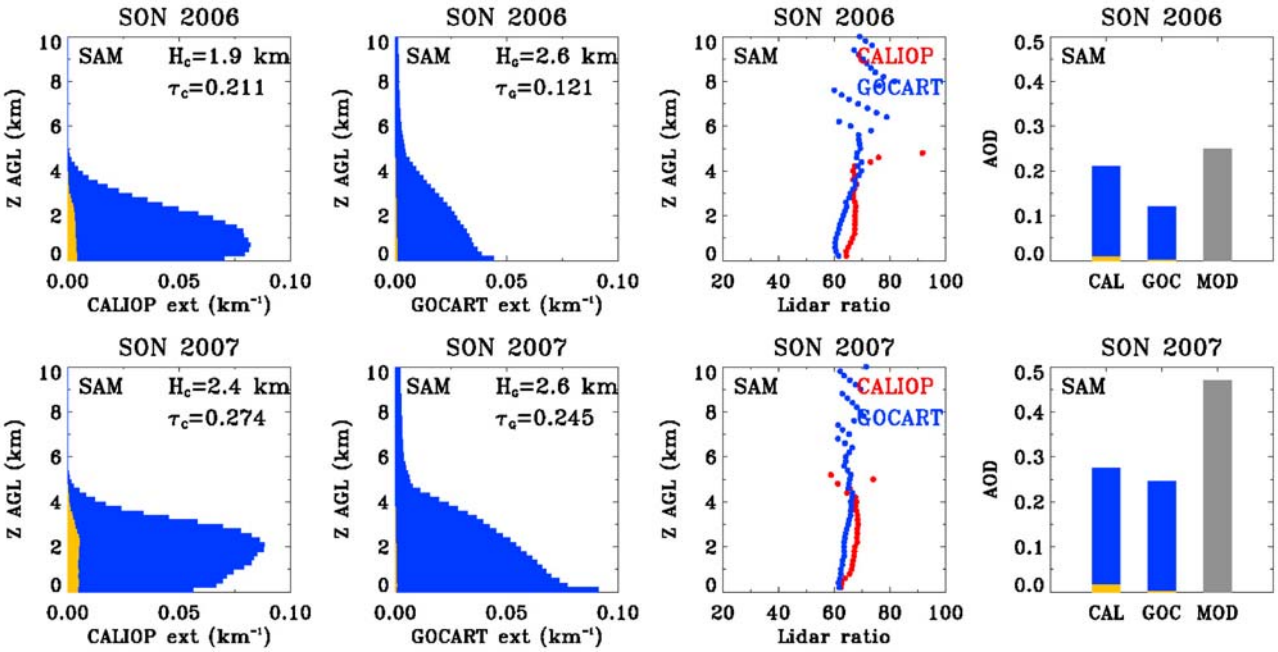

Figure 14. Same as Figure 7 but over South America (SAM) and for SON 2006 and SON 2007.

[42] 4. CALIOP observation and GOCART model agree in the estimated magnitude and seasonal variations of Saharan dust contribution to the aerosol extinction in the Sahel region.

[43] 5. For the aerosol lidar ratio, CALIOP observation generally agrees with GOCART model within 30%, except over Indian subcontinent and in the marine ABL of northwestern Pacific and midlatitude North Atlantic during some seasons. The best agreement occurs in biomass burning regions.

[44] Several major differences between satellite observations and GOCART model are also identified, including:

[45] 1. Over Indian sub-continent, GOCART model tends to substantially underestimate the magnitude of aerosol extinction, as compared to MODIS, CALIOP, and AERONET observations. Although CALIOP observations seemingly suggest the underestimate resulting mainly from dust, a robust attribution of uncertainties to aerosol types requires a better separation of dust from non-dust aerosol in the future.

[46] 2. In dust source regions, GOCART extinction is generally larger than CALIOP observation by a factor of 2 or more. This large difference could result from possible CALIOP misclassification of heavy dust as clouds and missed ABL dust due to the attenuation of signal, and/or possible overestimate of dust emissions by GOCART.

[47] 3. For aerosol outflows from North America and East Asia, CALIOP observations are much weaker in magnitude and much more concentrated in the lower atmosphere than that suggested by GOCART model and MODIS AOD observation. The differences are likely to result from uncertainties associated with all data sets. MODIS AOD retrievals may have high bias resulting from cloud contamination and presence of non-spherical dust. The GOCART model may overestimate dust emissions and the transport of ABL aerosol to the FA. For CALIOP measurements, one probable reason is that current aerosol classification algorithm tends to misclassify ABL outflow of spherical continental aerosol as marine aerosol and hence substantially underestimate extinction because of the assignment of too low lidar ratio. Another probable reason is that CALIOP's cloud-free observations, limited by the 16-day repeating cycle and high cloudiness in the regions, may have missed some important transport events associated with cloud systems, because midlatitude cyclones are the most effective mechanism that pumps ABL aerosol to the FA for the subsequent intercontinental transport.

[48] 4. Over tropical biomass burning regions, GOCART model simulates higher aerosol loading in Sahel in winter but lower aerosol loading over South America in austral spring of 2006 than satellite observations. Year-to-year variations of biomass burning smoke over South America as revealed by CALIOP observations are generally much smaller than that suggested by the GOCART model and MODIS retrieval, which would be partly linked to more undetectable ABL smoke due to stronger laser attenuation in heavier smoke year.

[49] Future efforts are needed to extend current analysis to above-cloud aerosol extinction that are essential to estimating the aerosol direct radiative forcing in cloudy conditions [*Chand et al.*, 2009]. Possible daytime and nighttime differences in aerosol extinction profile need to be examined. A more robust separation of dust from non-dust aerosol is needed, such as the use of PDR to partition the detected aerosol layer into dust and non-dust components in dust-pollution mixture regions. This would be extremely helpful in effectively guiding the improvement of models. Built on detail analysis of CALIOP and GOCART extinction profiles, much effort is needed to extend previous MODIS-GOCART integration framework [*Yu et al.*, 2003] by incorporating CALIOP vertical profiles and hence to achieve observation-based estimates of altitude-resolved aerosol direct radiative forcing.

[50] We have learned from this study that several aspects of model simulations and satellite observations need to be improved. Current CALIOP observations of aerosol extinction profile have large uncertainties because of the sensitivity of lidar, uncertainties associated with aerosol type and lidar ratio determination, feature misclassifications, and the saturation of laser light. While ongoing, dedicated effort of improving CALIOP retrieval algorithms will produce aerosol extinction profiles with much improved quality, the HSRL technology that directly measures extinction profiles with a high sensitivity [*Burton et al.*, 2010] could be employed in future satellite missions. This study and other model evaluation effort [e.g., *Chin et al.*, 2009] clearly show that the model tends to underestimate tropical biomass burning smoke emissions and pollution and/or dust emissions in Indian subcontinent. Continued effort in improving emission inventories is needed. A significant fraction of wildfire smoke could be injected into the FA [*Kahn et al.*, 2008], which needs to be accounted for in the global model, for example through implementing a sub-grid plume rise model [*Freitas et al.*, 2007]. Parallel to emission improvements, it is also essential to improve such atmospheric processes as convection, wet removal, transport, chemistry, and aerosol microphysics. Comparing CALIOP observations with multiple models could provide more insights for guiding improvements of models and satellite retrievals than a single model evaluation as in this study does. It is thus worth to conduct similar comparisons between CALIOP observations and other aerosol models, such as a group of AeroCom models [*Schulz et al.*, 2006; *Textor et al.*, 2006]. The data screening and analysis approaches developed in this study can be applied to such analyses.

[51] **Acknowledgments.** This research was supported by the Atmospheric Chemistry Modeling and Analysis Program (ACMAP), CALIPSO program and EOS program of NASA. We are grateful to Lorraine Remer for insightful comments. We thank the reviewers for their comments, which helped us improve the manuscript. The CALIPSO data were obtained from the NASA Langley Research Center Atmospheric Sciences Data Center.

References

Al-Saadi, J., et al. (2005), Improving national air quality forecasts with satellite aerosol observations, *Bull. Am. Meteorol. Soc.*, *86*, 1249–1261, doi:10.1175/BAMS-86-9-1249.

Andreae, M. O., D. Rosenfeld, P. Artaxo, A. A. Costa, G. P. Frank, K. M. Longo, and M. A. F. Silva-Dias (2004), Smoking rain clouds over the Amazon, *Science*, *303*, 1337–1342, doi:10.1126/science.1092779.

Barnaba, F., and G. P. Gobbi (2001), Lidar estimation of tropospheric aerosol extinction, surface area and volume: Maritime and desert dust cases, *J. Geophys. Res.*, *106*, 3005–3018, doi:10.1029/2000JD900492.

Burton, S. P., et al. (2010), Using airborne high spectral resolution lidar data to evaluate combined active plus passive retrievals of aerosol extinction profiles, *J. Geophys. Res.*, *115*, D00H15, doi:10.1029/2009JD012130.

Chand, D., R. Wood, T. L. Anderson, S. K. Satheesh, and R. J. Charlson (2009), Satellite-derived direct radiative effect of aerosols dependent on cloud cover, *Nat. Geosci.*, *2*, 181–184, doi:10.1038/ngeo437.

Chiapello, I., et al. (1997), Origins of African dust transported over the northeastern tropical Atlantic, *J. Geophys. Res.*, *102*, 13,701–13,709, doi:10.1029/97JD00259.

Chin, M., R. B. Rood, S.-J. Lin, J.-F. Muller, and A. M. Thompson (2000a), Atmospheric sulfur cycle simulated in the global model GOCART: Model description and global properties, *J. Geophys. Res.*, *105*, 24,671–24,687.

Chin, M., et al. (2000b), Atmospheric sulfur cycle in the global model GOCART: Comparison with field observations and regional budgets, *J. Geophys. Res.*, *105*, 24,689–24,712.

Chin, M., et al. (2002), Tropospheric aerosol optical thickness from the GOCART model and comparisons with satellite and sunphotometer measurements, *J. Atmos. Sci.*, *59*, 461–483, doi:10.1175/1520-0469(2002)059<0461:TAOTFT>2.0.CO;2.

Chin, M., P. Ginoux, R. Lucchesi, B. Huebert, R. Weber, T. Anderson, S. Masonis, B. Blomquist, A. Bandy, and D. Thornton (2003), A global model forecast for the ACE-Asia field experiment, *J. Geophys. Res.*, *108*(D23), 8654, doi:10.1029/2003JD003642.

Chin, M., A. Chu, R. Levy, L. Remer, Y. Kaufman, B. Holben, T. Eck, P. Ginoux, and Q. Gao (2004), Aerosol composition and distributions in the northern hemisphere during ACE-Asia: Results from global model, satellite observations, and surface sunphotometer measurements, *J. Geophys. Res.*, *109*, D23S90, doi:10.1029/2004JD004829.

Chin, M., T. Diehl, P. Ginoux, and W. Malm (2007), Intercontinental transport of pollution and dust aerosols: Implications for regional air quality, *Atmos. Chem. Phys.*, *7*, 5501–5517, doi:10.5194/acp-7-5501-2007.

Chin, M., T. Diehl, O. Dubovik, T. F. Eck, B. N. Holben, A. Sinuyk, and D. G. Streets (2009), Light absorption by pollution, dust, and biomass burning aerosols: A global model study and evaluation with AERONET measurements, *Ann. Geophys.*, *27*, 3439–3464, doi:10.5194/angeo-27-3439-2009.

De Tomasi, F., A. Blanco, and M. Perrone (2003), Raman lidar monitoring of extinction and backscattering of African dust layers and dust characterization, *Appl. Opt.*, *42*, 1699–1709, doi:10.1364/AO.42.001699.

Esselborn, M., M. Wirth, A. Fix, B. Weinzierl, K. Rasp, M. Tesche, and A. Petzold (2009), Spatial distribution and optical properties of Saharan dust observed by airborne high spectral resolution lidar during SAMUM 2006, *Tellus, Ser. B*, *61*, 131–143.

Freitas, S. R., K. M. Longo, R. Chatfield, D. Latham, M. A. F. Silva Dias, M. O. Andreae, E. Prins, J. C. Santos, R. Gielow, and J. A. Carvalho Jr. (2007), Including the sub-grid scale plume rise of vegetation fires in low resolution atmospheric transport models, *Atmos. Chem. Phys.*, *7*, 3385–3398, doi:10.5194/acp-7-3385-2007.

Ginoux, P., M. Chin, I. Tegen, J. Prospero, B. Holben, O. Dubovik, and S.-J. Lin (2001), Sources and distributions of dust aerosols simulated with the GOCART model, *J. Geophys. Res.*, *106*, 20,255–20,273, doi:10.1029/2000JD000053.

Ginoux, P., J. Prospero, O. Torres, and M. Chin (2004), Long-term simulation of dust distribution with the GOCART model: Correlation with the North Atlantic Oscillation, *Environ. Model. Softw.*, *19*, 113–128, doi:10.1016/S1364-8152(03)00114-2.

Hayasaka, T., S. Satake, A. Shimizu, N. Sugimoto, I. Matsui, K. Aoki, and Y. Muraji (2007), Vertical distribution and optical properties of aerosols observed over Japan during the Atmospheric Brown Clouds-East Asia Regional Experiment 2005, *J. Geophys. Res.*, *112*, D22S35, doi:10.1029/2006JD008086.

Kahn, R. A., B. Gaitley, J. Martonchik, D. Diner, K. Crean, and B. Holben (2005), MISR global aerosol optical depth validation based on two years of coincident AERONET observations, *J. Geophys. Res.*, *110*, D10S04, doi:10.1029/2004JD004706.

Kahn, R. A., W.-H. Li, C. Moroney, D. J. Diner, J. V. Martonchik, and E. Fishbein (2007), Aerosol source plume physical characteristics from space-based multiangle imaging, *J. Geophys. Res.*, *112*, D11205, doi:10.1029/2006JD007647.

Kahn, R., Y. Chen, D. Nelson, F.-Y. Leung, Q. Li, D. Diner, and J. Logan (2008), Wildfire Smoke Injection Heights: Two perspectives from Space, *Geophys. Res. Lett.*, *35*, L04809, doi:10.1029/2007GL032165.

Kalu, A. E. (1979), The African dust plume: Its characteristics and propagation across West Africa in winter, *SCOPE*, *14*, 95–118.

Kaufman, Y. J., et al. (2005), Dust transport and deposition observed from the Terra-Moderate Resolution Imaging Spectroradiometer (MODIS) spacecraft over the Atlantic Ocean, *J. Geophys. Res.*, *110*, D10S12, doi:10.1029/2003JD004436.

Kim, S.-W., S.-C. Yoon, J. Kim, and S.-Y. Kim (2007), Seasonal and monthly variations of columnar aerosol optical properties over east Asia determined from multi-year MODIS, LIDAR, and AERONET Sun/sky radiometer measurements, *Atmos. Environ.*, *41*, 1634–1651, doi:10.1016/j.atmosenv.2006.10.044.

Kim, S.-W., S. Berthier, J.-C. Raut, P. Chazette, E. Dulac, and S.-C. Yoon (2008), Validation of aerosol and cloud layer structures from the spaceborne lidar CALIOP using a ground-based lidar in Seoul, Korea, *Atmos. Chem. Phys.*, *8*, 3705–3720, doi:10.5194/acp-8-3705-2008.

Kinne, S., et al. (2006), An AeroCom initial assessment—Optical properties in aerosol component modules of global models, *Atmos. Chem. Phys.*, *6*, 1815–1834, doi:10.5194/acp-6-1815-2006.

Koren, I., L. A. Remer, and K. Longo (2007), Reversal of trend of biomass burning in the Amazon, *Geophys. Res. Lett.*, *34*, L20404, doi:10.1029/2007GL031530.

Levy, R., L. A. Remer, S. Mattoo, E. Vermote, and Y. J. Kaufman (2007), Second-generation algorithm for retrieving aerosol properties over land

from MODIS spectral reflectance, *J. Geophys. Res.*, *112*, D13211, doi:10.1029/2006JD007811.

Liu, D., Z. Wang, Z. Liu, D. Winker, and C. Trepte (2008), A height resolved global view of dust aerosols from the first year CALIPSO lidar measurements, *J. Geophys. Res.*, *113*, D16214, doi:10.1029/2007JD009776.

Liu, Z., N. Sugimoto, and T. Murayama (2002), Extinction-to-backscatter ratio of Asian dust observed with high-spectral-resolution lidar and Raman lidar, *Appl. Opt.*, *41*, 2760–2767, doi:10.1364/AO.41.002760.

Liu, Z., et al. (2008), CALIPSO lidar observations of the optical properties of Saharan dust: A case study of long-range transport, *J. Geophys. Res.*, *113*, D07207, doi:10.1029/2007JD008878.

Liu, Z., et al. (2009), The CALIPSO lidar cloud and aerosol discrimination: Version 2 algorithm and initial assessment of performance, *J. Atmos. Oceanic Technol.*, *26*, 1198-1213, doi:10.1175/2009JTECHA1229.1.

Lohmann, U., et al. (2001), Comparisons of the vertical distribution of sulfur species from models participated in COSAM exercise with observations, *Tellus, Ser. B*, *53*, 646–672.

Mattis, I., A. Ansmann, D. Müller, U. Wandinger, and D. Althausen (2002), Dual-wavelength Raman lidar observations of the extinction-to-backscatter ratio of Saharan dust, *Geophys. Res. Lett.*, *29*(9), 1306, doi:10.1029/2002GL014721.

Müller, D., A. Ansmann, I. Mattis, M. Tesche, U. Wandinger, D. Althausen, and G. Pisani (2007), Aerosol-type-dependent lidar ratios observed with Raman lidar, *J. Geophys. Res.*, *112*, D16202, doi:10.1029/2006JD008292.

Murayama, T., et al. (2001), Ground-based network observation of Asian dust events of April 1998 in east Asia, *J. Geophys. Res.*, *106*, 18,345–18,360, doi:10.1029/2000JD900554.

Nakajima, T., et al. (2007), Overview of the Atmospheric Brown Cloud East Asia Regional Experiment 2005 and a study of the aerosol direct radiative forcing in East Asia, *J. Geophys. Res.*, *112*, D24S91, doi:10.1029/2007JD009009.

Omar, A., et al. (2009), The CALIPSO automated aerosol classification and lidar ratio selection algorithm, *J. Atmos. Oceanic Technol.*, *26*, 1994-2014, doi:10.1175/2009JTECHA1231.1.

Pierangelo, C., A. Chédin, S. Heilliette, N. Jacquinet-Husson, and R. Armante (2004), Dust altitude and infrared optical depth from AIRS, *Atmos. Chem. Phys.*, *4*, 1813–1822, doi:10.5194/acp-4-1813-2004.

Remer, L. A., and Y. J. Kaufman (2006), Aerosol direct radiative effect at the top of the atmosphere over cloud free ocean derived from four years of MODIS data, *Atmos. Chem. Phys.*, *6*, 237–253, doi:10.5194/acp-6-237-2006.

Remer, L. A., et al. (2005), The MODIS aerosol algorithm, products, and validation, *J. Atmos. Sci.*, *62*, 947–973, doi:10.1175/JAS3385.1.

Remer, L. A., et al. (2008), An emerging aerosol climatology from the MODIS satellite sensors, *J. Geophys. Res.*, *113*, D14S07, doi:10.1029/2007JD009661.

Rudich, Y., Y. J. Kaufman, U. Dayan, H. Yu, and R. G. Kleidman (2008), Estimation of transboundary transport of pollution aerosols by remote sensing in the eastern Mediterranean, *J. Geophys. Res.*, *113*, D14S13, doi:10.1029/2007JD009601.

Schulz, M., et al. (2006), Radiative forcing by aerosols as derived from the AeroCom present-day and pre-industrial simulations, *Atmos. Chem. Phys.*, *6*, 5225–5246, doi:10.5194/acp-6-5225-2006.

Shimizu, A., et al. (2004), Continuous observations of Asian dust and other aerosols by polarization lidars in China and Japan during ACE-Asia, *J. Geophys. Res.*, *109*, D19S17, doi:10.1029/2002JD003253.

Stohl, A., S. Eckhardt, C. Forster, P. James, and N. Spichtinger (2002), On the pathways and timescales of intercontinental air pollution transport, *J. Geophys. Res.*, *107*(D23), 4684, doi:10.1029/2001JD001396.

Tesche, M., et al. (2009), Vertical profiles of Saharan dust with Raman lidars and airborne HSRL in southern Morocco during SAMUM, *Tellus, Ser. B*, *61*, 144–164.

Textor, C., et al. (2006), Analysis and quantification of the diversities of aerosol life cycles within AeroCom, *Atmos. Chem. Phys.*, *6*, 1777–1813, doi:10.5194/acp-6-1777-2006.

Winker, D. M., and M. T. Osborn (1992), Preliminary analysis of observations of the Pinatubo volcanic plume with a polarization-sensitive lidar, *Geophys. Res. Lett.*, *19*, 171–174, doi:10.1029/91GL02866.

Winker, D. M., J. Pelon, and M. P. McCormick (2003), The CALIPSO mission: Spaceborne lidar for observations of aerosols and clouds, *Proc. SPIE Int. Soc. Opt. Eng.*, *4893*, 1–11.

Winker, D., W. H. Hunt, and M. J. McGill (2007), Initial performance assessment of CALIOP, *Geophys. Res. Lett.*, *34*, L19803, doi:10.1029/2007GL030135.

Winker, D. M., M. A. Vaughan, A. Omar, Y. Hu, K. A. Powell, Z. Liu, W. H. Hunt, and S. A. Young (2009), Overview of the CALIPSO mission and CALIOP data processing algorithms, *J. Atmos. Oceanic Technol.*, *26*, 2310-2323, doi:10.1175/2009JTECHA1281.1.

Young, S. A., and M. A. Vaughan (2009), The retrieval of profiles of particulate extinction from Cloud Aerosol Lidar Infrared Pathfinder Satellite Observations (CALIPSO) data: Algorithm description, *J. Atmos. Oceanic Technol.*, *26*, 1105-1119, doi:10.1175/2008JTECHA1221.1.

Yu, H., R. E. Dickinson, M. Chin, Y. J. Kaufman, B. N. Holben, I. V. Geogdzhayev, and M. I. Mishchenko (2003), Annual cycle of global distributions of aerosol optical depth from integration of MODIS retrievals and GOCART model simulations, *J. Geophys. Res.*, *108*(D3), 4128, doi:10.1029/2002JD002717.

Yu, H., R. E. Dickinson, M. Chin, Y. J. Kaufman, M. Zhou, L. Zhou, Y. Tian, O. Dubovik, and B. N. Holben (2004), The direct radiative effect of aerosols as determined from a combination of MODIS retrievals and GOCART simulations, *J. Geophys. Res.*, *109*, D03206, doi:10.1029/2003JD003914.

Yu, H., et al. (2006), A review of measurement-based assessments of the aerosol direct radiative effect and forcing, *Atmos. Chem. Phys.*, *6*, 613–666, doi:10.5194/acp-6-613-2006.

Yu, H., R. Fu, R. E. Dickinson, Y. Zhang, M. Chen, and H. Wang (2007), Interannual variability of smoke and warm cloud relationships in the Amazon as inferred from MODIS retrievals, *Remote Sens. Environ.*, *111*, 435–449, doi:10.1016/j.rse.2007.04.003.

Yu, H., L. A. Remer, M. Chin, H. Bian, R. Kleidman, and T. Diehl (2008), A satellite-based assessment of trans-Pacific transport of pollution aerosol, *J. Geophys. Res.*, *113*, D14S12, doi:10.1029/2007JD009349.

Yu, H., M. Chin, L. A. Remer, R. G. Kleidman, N. Bellouin, H. Bian, and T. Diehl (2009), Variability of marine aerosol fine-mode fraction and estimates of anthropogenic aerosol component over cloud-free oceans from the Moderate resolution Imaging Spectroradiometer (MODIS), *J. Geophys. Res.*, *114*, D10206, doi:10.1029/2008JD010648.

M. Chin, Laboratory for Atmospheres, NASA Goddard Space Flight Center, Greenbelt, MD 20771-0001, USA.

T. Diehl, Goddard Earth Science and Technology Center, University of Maryland Baltimore County, Baltimore, MD 21228, USA.

C. Kittaka, A. H. Omar, and D. M. Winker, NASA Langley Research Center, Hampton, VA 23681, USA.

Z. Liu, National Institute of Aerospace, Hampton, VA 23666, USA.

H. Yu, Earth System Science Interdisciplinary Center, University of Maryland, College Park, MD 20740, USA. (hongbin.yu-1@nasa.gov)